Vibration Analysis for Turbomachinery

Ed Wilcox
Consulting Machinery Engineer
Chevron Energy Technology Company
Houston, TX

Ed Wilcox is a Consulting Machinery Engineer with the Energy Technology Company (ETC) of Chevron. Prior to this he worked for Conoco and Lyondell Chemical as a machinery engineer. He has a BSME degree from the University of Missouri-Rolla and an MSME degree from Oklahoma State University.   He is a Vibration Institute Category IV Vibration Specialist and a registered Professional Engineer in the State of Oklahoma. Mr. Wilcox has authored multiple papers in the areas of rotordynamics, vibration analysis, and performance testing at both the Texas A&M Turbomachinery and Pump Symposia, along with several magazine articles.

ABSTRACT

Turbomachinery requires a higher level of vibration analysis than general purpose machinery. This includes identifying natural frequencies or modes of a system to determine if a potential resonance occurs. The complexity of turbomachinery requires this higher level of vibration analysis, which includes understanding the importance of transient data (i.e. start-up/shutdown), the role of rotordynamics, advanced signal processing, and many other concepts. Likewise, a different array of plotting configurations is required to extract the necessary data for an accurate assessment of the machinery (i.e. Bode, Nyquist, Waterfall, Cascade, shaft centerline, and time waveform plots). An essential part of machinery troubleshooting is using as measured vibration to "tune" a rotordynamic model so that it can accurately predict both stability and forced response changes. This will allow the engineer to make design changes to the equipment to potentially reduce the vibration to an acceptable level.

INTRODUCTION

The basics of vibration analysis include identifying the predominant frequency at which the vibration occurs and then determining what is the forcing function that is the cause. Reduction of the forcing function will many times reduce the amplitude of the component that is the concern. For this level of analysis the most common display format is the Fast Fourier Transform (FFT), more commonly known as the spectrum. The FFT is an excellent tool for doing just that, identifying individual frequencies.   For most general purpose equipment (i.e. pumps, fans, motors, etc… operating below 4000 rpm) the FFT can be used to identify and solve a vast majority of machinery issues.

One of the most difficult concepts to overcome in vibration analysis is that regardless of source of vibration, many vibration problems have one thing in common, they all have a synchronous (i.e. 1x) component. There are countless vibration troubleshooting charts published in the industry that list different causes of vibration and the subsequent source of excitation. However, if you review those charts, you will notice that 70-80% of the sources all list 1x vibration as a symptom.

This tutorial will give an explanation of these higher level concepts and the importance of the different plotting options. Strengths and weaknesses of shaft proximity probes are discussed briefly to ensure that the reader appreciate the limitations. The importance of the relative location of the rotor's natural frequencies to the operating speed will be covered and how this may change the produced vibration. To bring all of these concepts into focus, multiple case studies will be reviewed showing the problem, the solution methodology, the analysis, and the results. The case studies will include: high transient vibration on a high pressure barrel compressor, load induced high vibration on a large frame gas turbine generator, high synchronous vibration of a high speed steam turbine, sub-synchronous instability of a centrifugal compressor, unbalance problems on a refinery wet gas compressor, and near resonance operation of an electrical generator.

WHAT IS NOT COVERED

This tutorial does not cover the basics of vibration analysis. It is assumed that the reader already understands the concepts of amplitude, frequency, and phase of vibration. Additionally, terms such as peak, peak-peak, 1x, 2x, and synchronous vibration will be used but not explained. For further background on general vibration analysis, see Ref[1,2,5,8]. This paper is focused on the analysis of turbomachinery vibration, but does not include any details around machinery protection requirements or hardware. This paper does not cover analysis of data from velocity or acceleration transducers. While this data can be important for analyzing some types of turbomachinery (aeroderivative gas turbines, gearboxes), the analysis concepts are well covered in the literature and not included here.

SHAFT DISPLACEMENT PROBES

Shaft displacement probes (non-contacting eddy current sensors) measure the displacement of the rotor or shaft typically adjacent to or inside a hydrodynamic journal bearing. Displacement probes are significantly different from the bearing or casing vibration measurements common on general purpose equipment. The nature of hydrodynamic bearings (both fixed and tilting pads) is such that the shaft can move substantially inside the bearing without transmitting a significant vibration to the bearing housing or casing. This is many times the result of very low rotor to casing mass ratios on turbomachinery

The basic configuration of a displacement probe is shown below in Figure 1. The system consists of a matched set of components

- Probe
- extension cable
- oscillator/demodulator (commonly called a proximeter).

The proximiter excites the probe with a RF signal at approximately 2 MHz. This produces a magnetic field at the tip of the probe, see Figure 2. The proximiter demodulates the signal from the probe and provides a modulated DC voltage which is directly proportional to the distance between the probe tip and the target (commonly called the "gap"). A plot of the probe output voltage versus gap in shown in Figure 3. The AC portion of the signal is directly proportional to the vibration of the rotor. Therefore the proximity probe can provide both rotor position as well as vibration(displacement), see Figure 4. The rotor position can be used to determine the average journal position in a radial bearing or the axial position in a thrust bearing. This is a very important diagnostic tool since a change in shaft position in a radial bearing may indicate a damaged bearing.
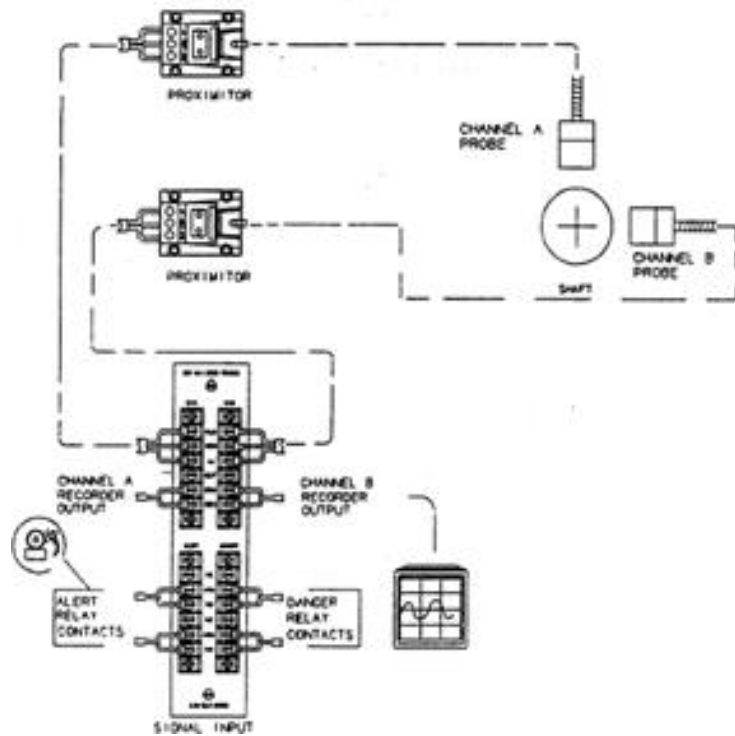
Figure 1. Eddy current probe/proximiter configuration (General Electric)
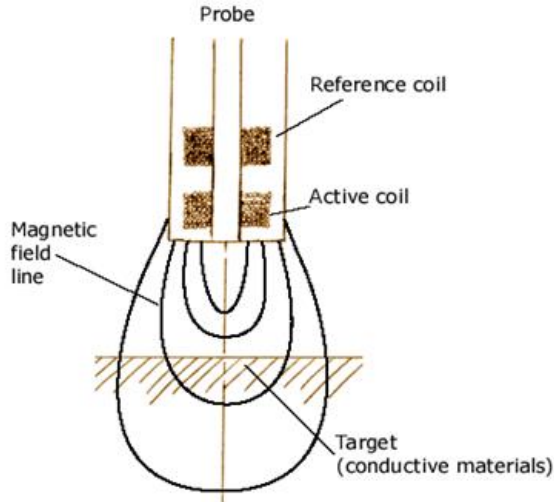
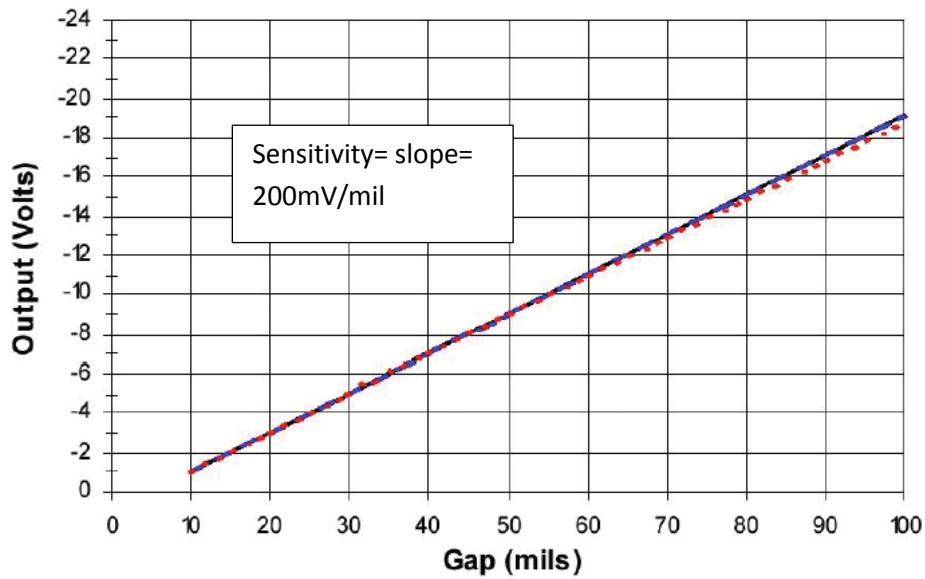*Figure 2. Illustration of proximity probe eddy current field(General Electric)*

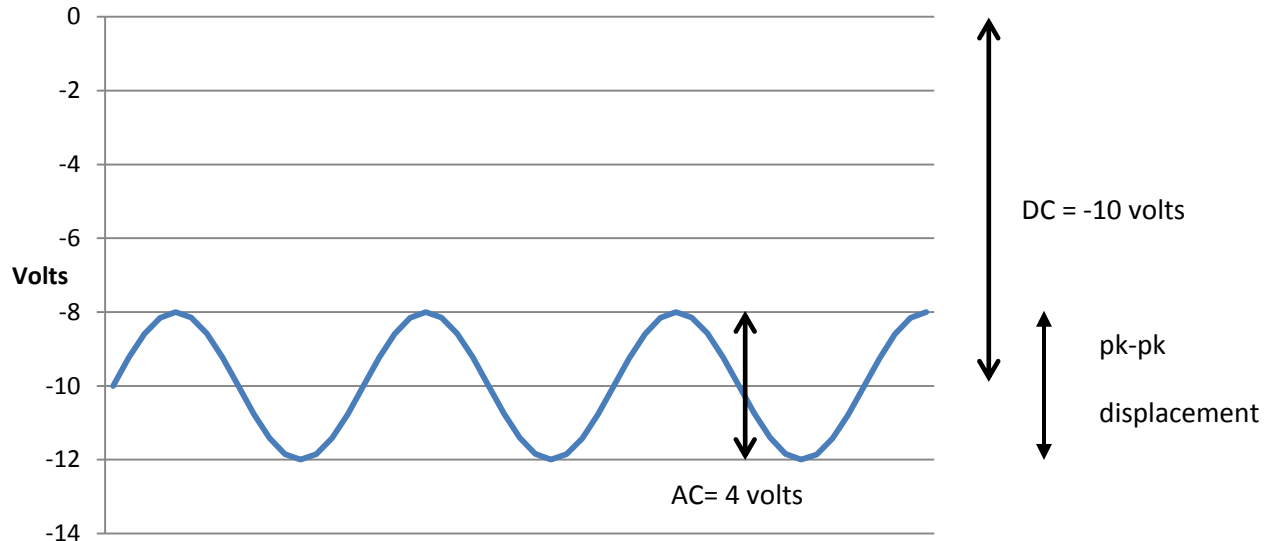*Figure 3. Typical proximity probe output voltage versus gap(mils) (General Electric)*

Figure 4. Typical proximity probe output showing gap(DC) and vibration(AC) components

The primary advantages of the proximity probe over other measurement types is that it provides the actual shaft displacement, not the vibration transmitted to some other part of the machinery. Additionally, displacement probes are very rugged and reliable if properly installed. Invariably, when a high vibration is encountered in machinery, one of the first questions by upper management is "is the vibration real?" (i.e. valid). With proximity probes, the vast majority of time the answer is "yes". While proximity probes are very rugged and reliable, just like any other condition monitoring device, they do have some potential short-comings. Some of these disadvantages of are:

- Target surface condition – imperfections in the target area of the rotor where the displacement probe reads are reported to the measuring device as displacement. The probe targets have to be kept free of scratches, corrosion, and other imperfections that will potentially cause false signals. An example of a proximity probe output where the target has a scratch is shown in Figure 5. Note that the vibration monitor cannot distinguish this defect from actual vibration. Similarly, the FFT will just show this defect as 1X vibration. The time waveform and orbit are the best diagnostic tools to identify such abnormalities. For this reason the probe target area must be protected during rotor repair and storage. Every senior machinery engineer has experienced the frustration of a damaged probe target area from someone's pocket knife or just simple corrosion. The solution to runout is vector compensation of the displacement data. This is accomplished by collecting a slow roll vector for each probe and subtracting the slow roll vector from the measured displacement vector. The slow roll vector is the actual displacement vector at a very low rotational speed where the shaft is just turning in the bearings (no actual vibration). It is should be noted, that since this is a vector subtraction, the magnitude of the resultant or compensated displacement vector is not always lower than the measured displacement, it just depends on the phase difference between the slow roll and

displacement vector (an example of this is provided in the next section). A more rigorous compensation of the vibration data is accomplished with actual waveform compensation, where a time waveform is recorded at low speed instead of just a vector. An example of a compensated time wave form is shown in Figure 6.
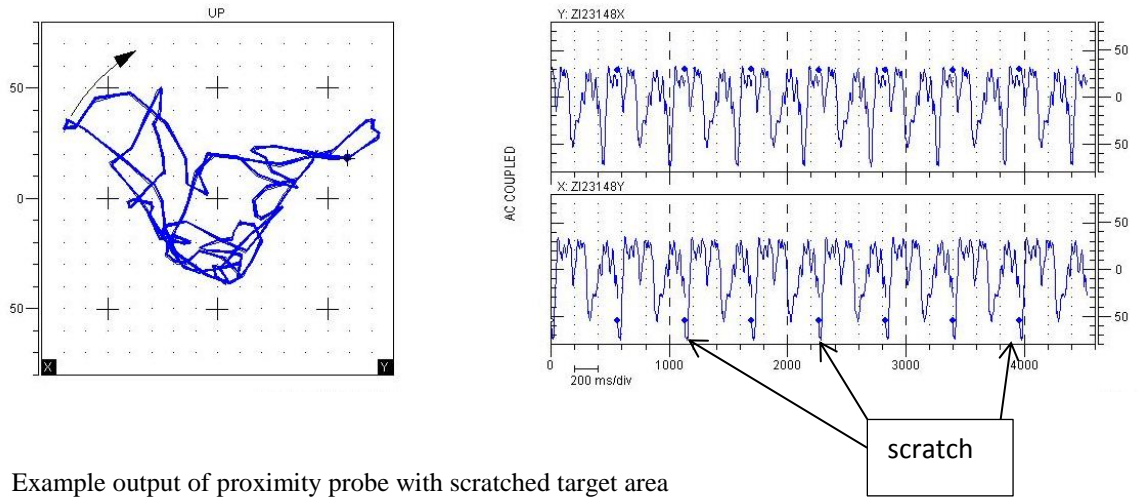

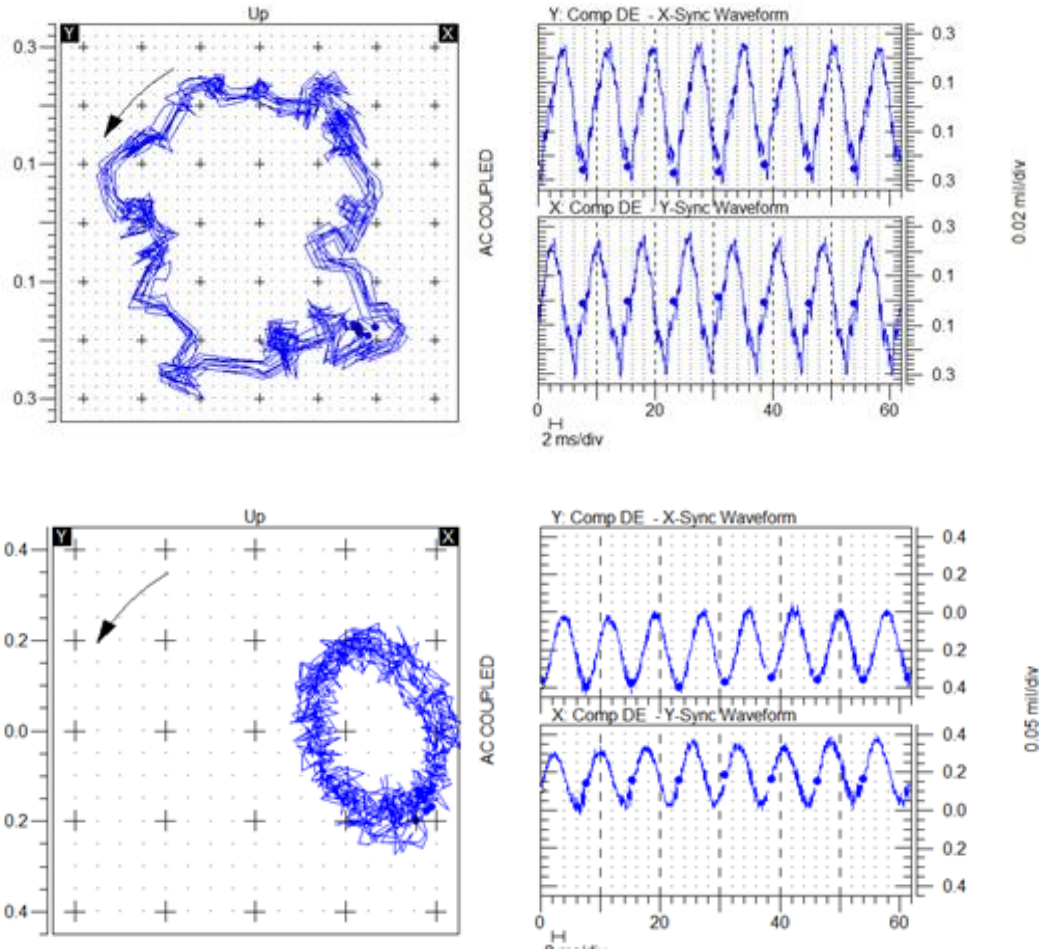Figure 5. Example output of proximity probe with scratched target area

Figure 6. Direct orbit (upper) and orbit with waveform compensation (lower)

- Magnetism – If the rotor has any residual magnetism, this may affect the probe readings and potentially cause runout similar to physical imperfections in the target surface described above. This is commonly referred to as "electrical runout" in the industry.

- Target material – the default shaft material for proximity probes is normally 4140 steel. Since the eddy currents are sensitive to the permeability and resistivity of the shaft material, any material other than 4000 series steels must be planned for in the design of the condition monitoring system. Some options include a steel coating in the probe target area or specific probes that are calibrated for the shaft material.

- Improper proximiter/cable/probe combinations - as mentioned above, the proximity probe system include three components(probe, extension cable, and proximiter). The cable on the probe itself is 1 m in length. The proximiter is tuned for a particular probe and extension cable length. Most proximiter probes are supplied in 1m, 5m, and 9m total length options (i.e. extension cable lengths of 0, 4, and 8 m respectively). If the extension cable is mis-matched with the incorrect proximiter it can cause erroneous results. Figure 7 shows three spectrums taken with an analyzer using a 1 m probe only, then 4 m, and 8 m extension cables. The proximiter was designed for the 1m probe (i.e. no extension cable). The author has also seen a centrifugal compressor factory acceptance test (FAT) where an incorrect extension cable/proximiter combination created a 2X peak that caused the OEM to suspect misalignment before determining the actual problem.

- Side wall interference - Because the eddy current is emitted from the tip of the probe, the probe tip must have a clearance that is equal to at least 3x the probe tip diameter to avoid side wall interference.
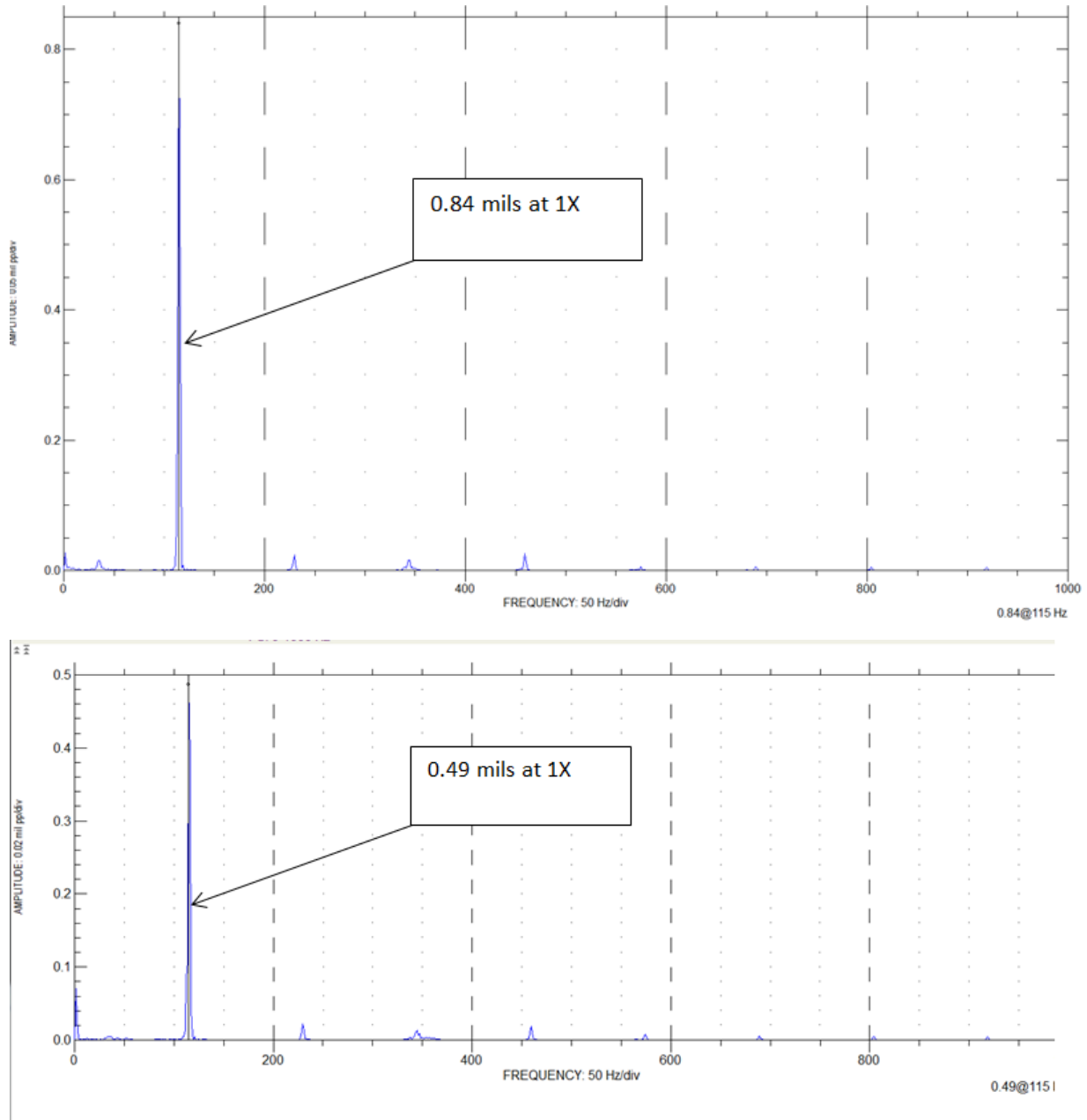

1.51 mils at 1X

FREQUENCY: 50 Hz/div

1.51@112.50 Hz
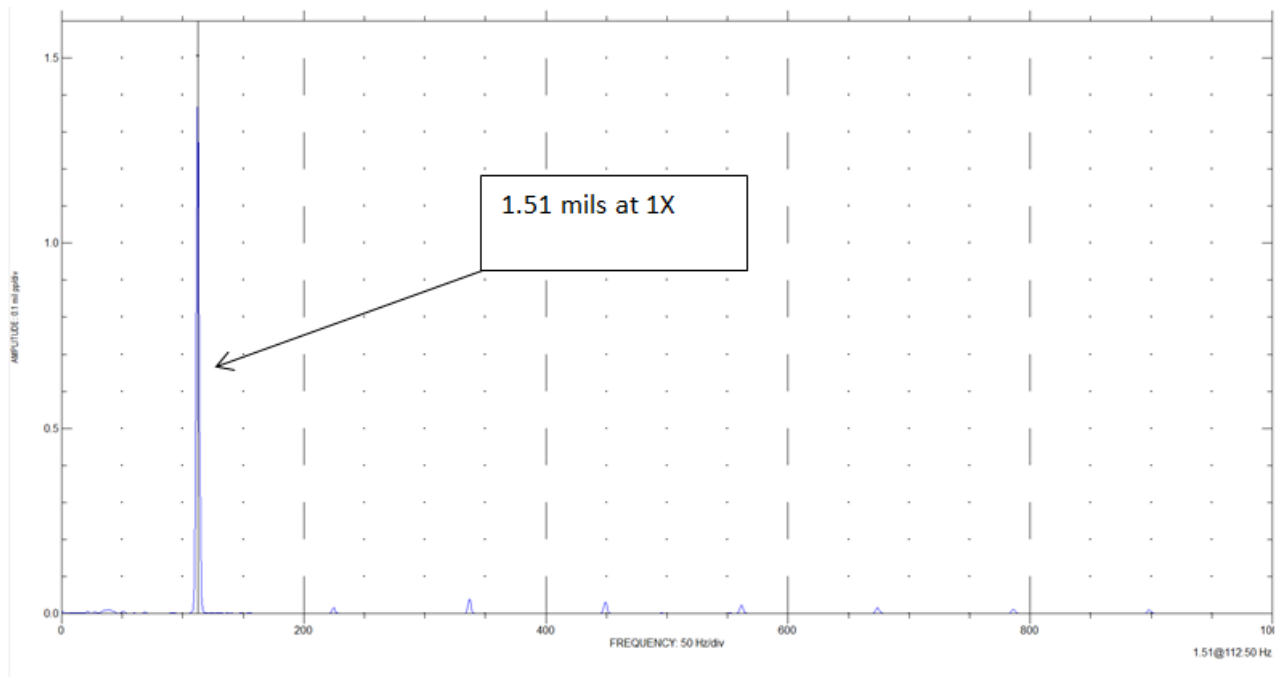
Figure 7. Spectrums taken with different extension cable lengths(none(top), 4m(middle), 8m(bottom)).

DATA DISPLAY FORMATS

Bode and Polar Plots

At the most basic level, the Bode plot is merely vibration amplitude and phase versus shaft speed, see Figure 8. However, it can potentially provide a wealth of information not available from steady state plots such as the FFT. The most common use of the Bode plot is the identification of natural frequencies present in the machinery. The most common of these are called "critical speeds" which occur when the shaft rotational speed coincides with a lateral mode and produces a resonance. This appears as an amplitude peak and phase shift in the Bode plot (approximately 3600 cpm in Figure 8). Identification of natural frequencies is especially critical in turbomachinery because unlike most general purpose equipment, they operate above or close to one if not more natural frequencies or modes. The Bode plot is most powerful in identifying high synchronous vibration. While overall vibration can be plotted versus shaft speed as well, the Bode plot is not really a tool for identifying non-synchronous vibration. This is a function that is best performed using a FFT in the form of either a cascade or waterfall plot, to be discussed later.

The importance of compensation and the affect it has on recorded vibration is shown in the Bode plot in Figure 8. As can be seen, the compensated vector magnitude (blue) starts at a zero value, in comparison to the un-compensated values that start at approximately 0.2 mils. The slow roll vector for this probe is approximately 0.22 mils at 21°. As mentioned above, it is extremely important to note that the compensated value is not always less than the raw value. As the phase of the synchronous vector changes, the vector subtraction both increases and decreaes the magnitude of the compensated vector.
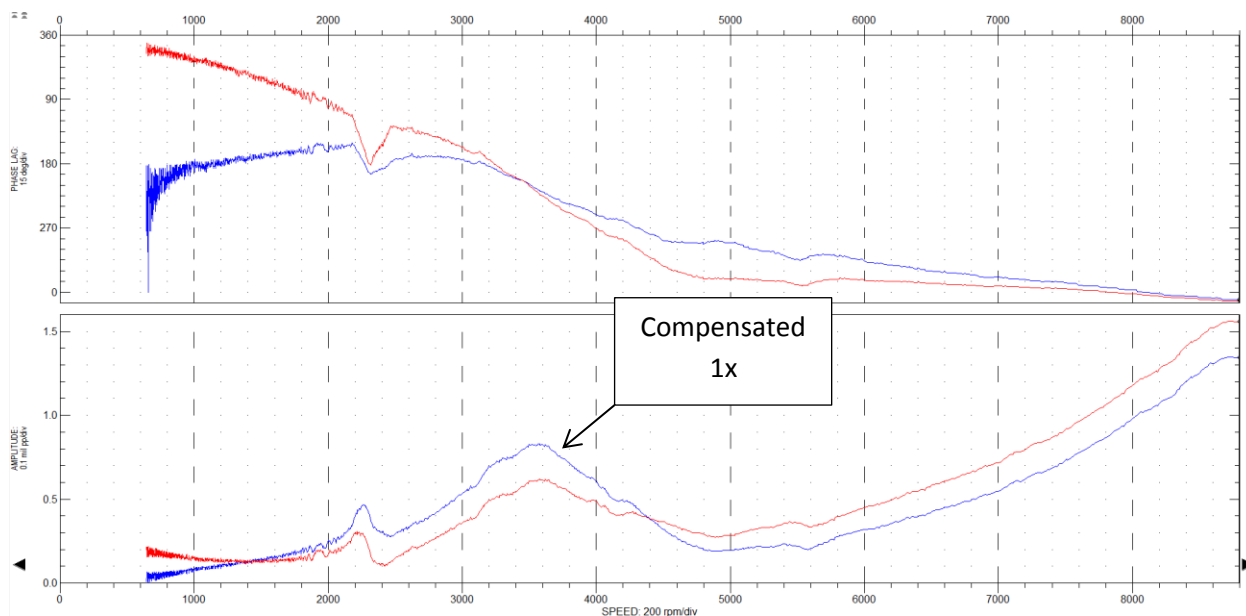

Figure 8. Bode plot showing both raw (red) and compensated (blue) synchronous vibration data

The polar plot presents the exact same data as the Bode plot, just in a different display format. In the polar plot the displacement vector magnitude is measured radially, from the center of the plot and the phase is plotted circumferentially. The same data from Figure 8 is plotted in Figure 9 below. A resonance is indicated in a polar plot by the speed at which amplitude is a maximum of a loop (i.e. approximately 180 degree phase shift). Additional background information about Bode and Polar plots are provided in Ref[4].
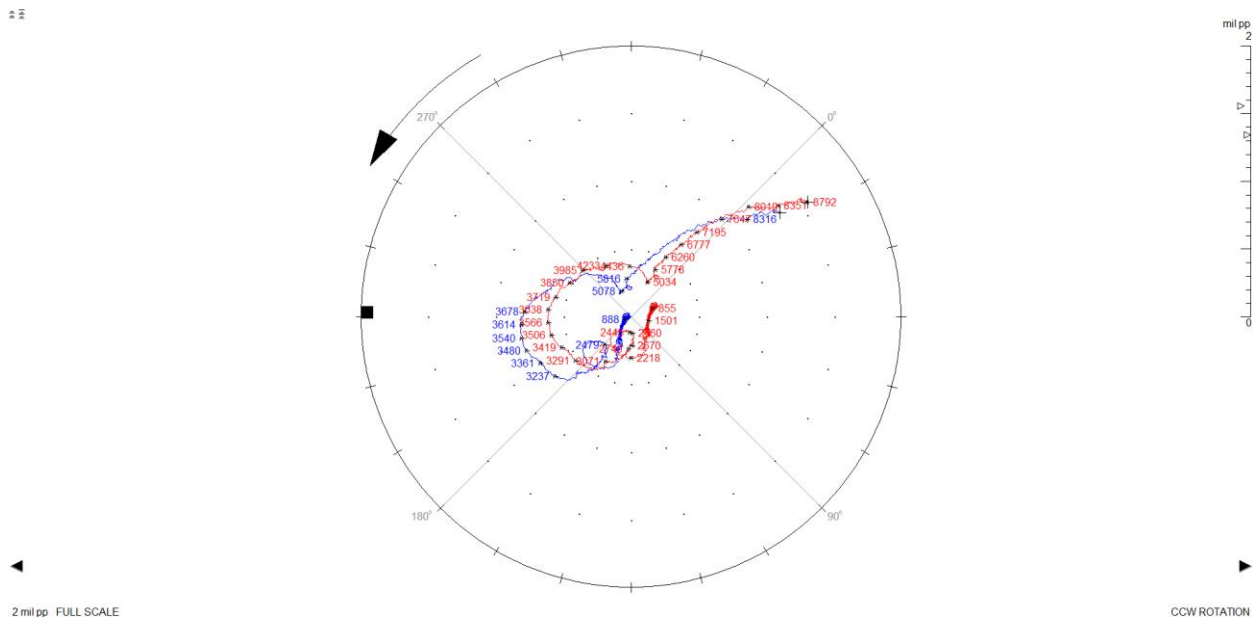
Figure 9. Polar plot showing both raw (red) and compensated (blue) synchronous vibration data (same data as Figure 8, just different format)

An example of the importance of identifying resonance conditions is shown in the Bode plot of a 4 pole generator in Figure 10a. As can be seen, the radial vibration is relatively low (1.121 mils synchronous) at the generator's operating speed (1800 rpm). However, as the speed of the generator is increased to approximately 20% over the synchronous operating speed, the magnitude of the vibration increases dramatically to over 10 mils. Undoubtedly, there is a lateral mode between 2200 and 2300 rpm on this particular machine. Note, that the phase change in the Bode plot appears to show the resonance at approximately 1800 rpm. However, review of the polar plot for the same date gives a better view of the phase change, indicating that at 2250 rpm the generator is right on top of a critical speed, see Figure 10b.

Since an electrical generator rarely operates above its synchronous speed, this would not appear to be a large concern. However, if the overall system stiffness were to be reduced in the future (i.e. the bearing clearance were to increase) then it is possible that this lateral mode could shift downward. The mode would not have to shift all the

way down to 1800 rpm to cause problems. If the mode just dropped to approximately 2000 rpm, the radial vibration at 1800 rpm might increase to approximately 5-6 mils on the skirt of the critical. This is an excellent example of the need to collect and store transient data during Factory Acceptance Testing (FAT) to be used in troubleshooting potential problems in the field.
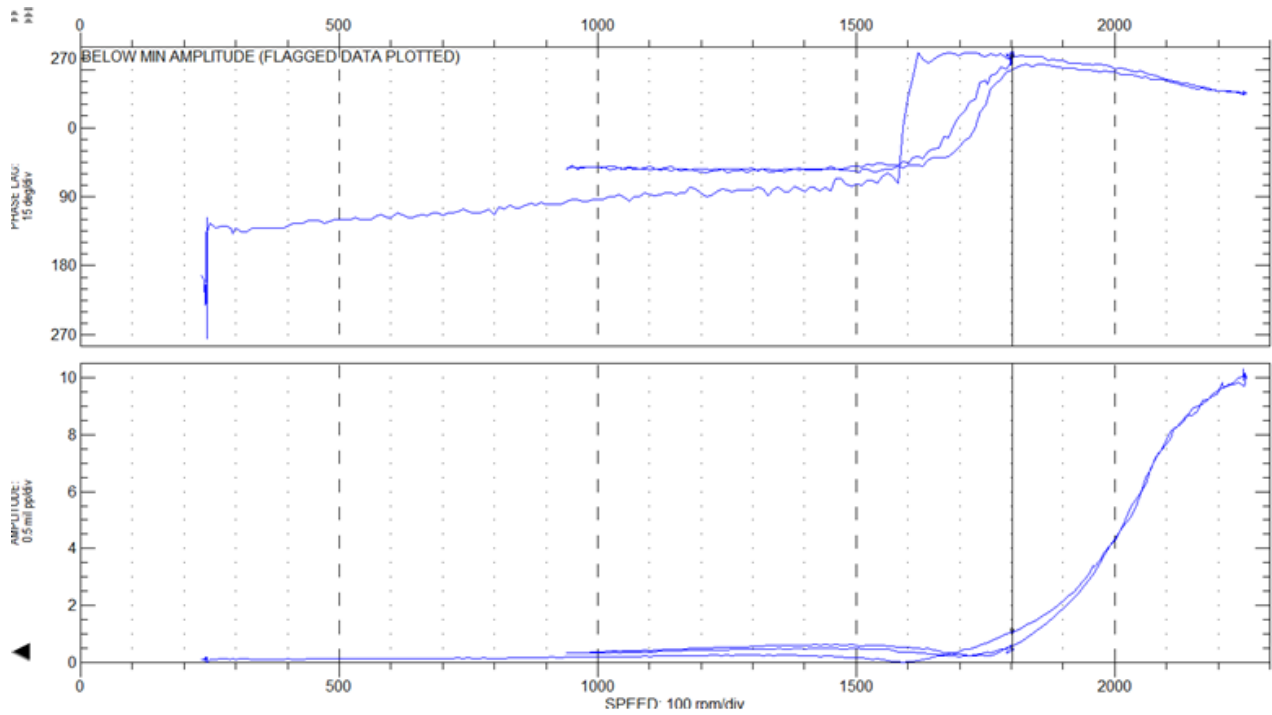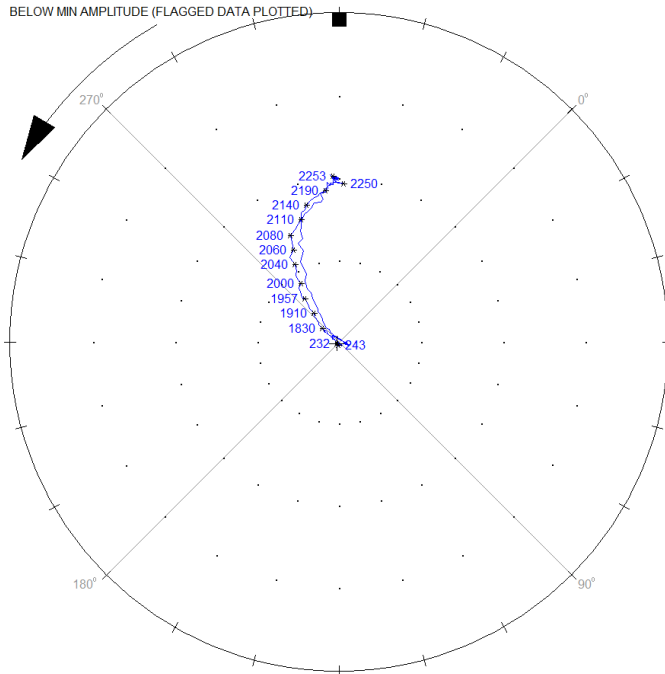

Figure 10a. Bode plot 4 pole generator FAT

Figure 10b. Polar plot of 4 pole generator FAT

One of the most basic concepts to understand is the relationship between the location of mass unbalance (heavy spot) and measured displacement (high spot) below, at, and above a critical speed, see Figure 11. Well below a rotor's critical speed, the high spot and heavy spot are very close together and the phase difference between the two is negligible. As the rotational speed of the machine increases, the force vector (caused by the heavy spot) begins leading the vibration. At the point of resonance, the force vector is leading the vibration by 90°. It should be noted that since velocity lags displacement by 90° the velocity vector is 180° opposite the force vector at resonance. This is very important because it indicates that the shaft stiffness (which acts on the displacement), cannot reduce the unbalance force at resonance. Only the velocity vector, which acts on the system damping can reduce the vibration produced by the force vector. For this reason, the measured response at resonance is a very strong indication of the damping present in the system, see Figure 12. As the rotational speed increases well above resonance, the force vector eventually leads the displacement vector by approximately 180°. The importance of this is that mass unbalance of the rotor is now 180° from the measured displacement. This is a result of the physical phenomena that the rotor whirls about its geometric center below the critical, but around its mass center above the critical.   Well above the rotor's critical the displacement approaches the unbalance level (i.e. d ->e). This is why many rotors operate at lower displacement levels above their 1st critical speed. This has the obvious affect that balance corrections (relative to the measured vibration) are made in the opposite location depending on if the rotor operates above or below, it's critical.   It should be remembered, that weight is always removed opposite the heavy spot, regardless of operating below or above the critical.
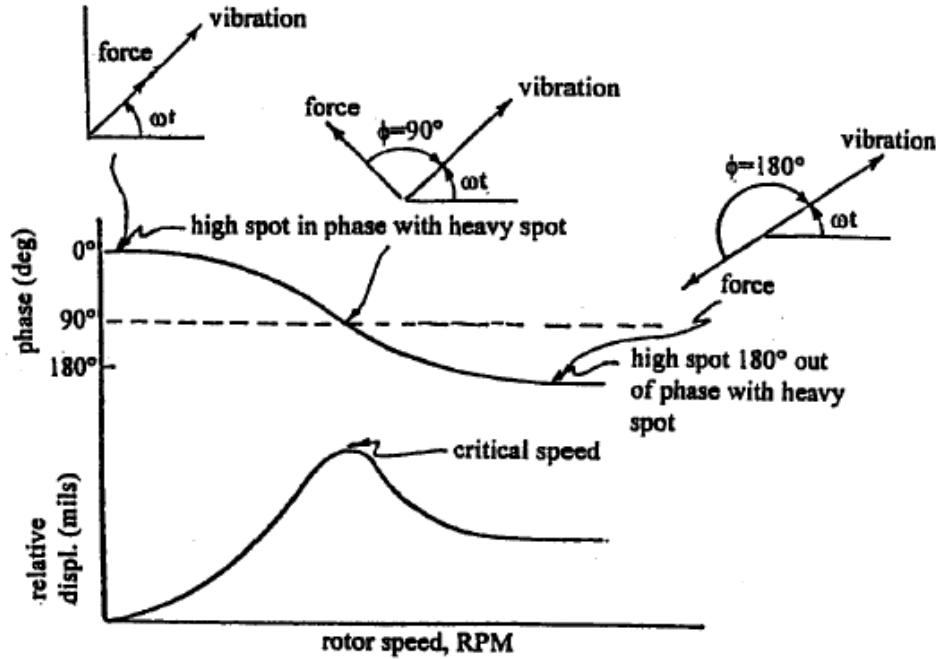
Figure 11. Relationship of high and heavy spot below, at, and above resonance (TPS)
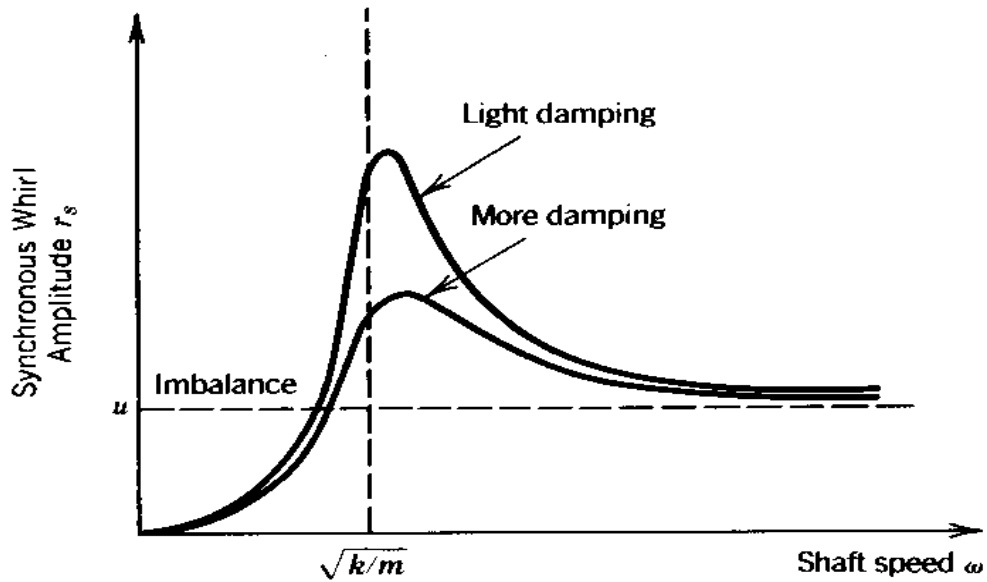

Figure 12. Amplitude response at resonance for different amounts of damping (TPS)

The synchronous amplification factor (AF) is a non-dimensional factor that is a strong indicator of the damping present in the rotor system. A common method of defining AF is the half-power method, see Figure 13 below. Most turbomachinery operate on hydrodynamic bearings of some type which provide a large amount of the damping present in the system. For this reason changes in AF normally indicate changes in the damping provided by the bearings, which can indicate damage to the bearings. If a tilt-pad style bearing has been damaged or "wiped", then the stiffness and damping characteristics are both normally reduced. However, it is very common for the damping to be reduced more than the stiffness, which results in an increase in AF. This is commonly referred to as a decrease in the "effective" damping. This can be used to distinguish between damaged bearings and other potential causes of high synchronous vibration, such as unbalance or misalignment.
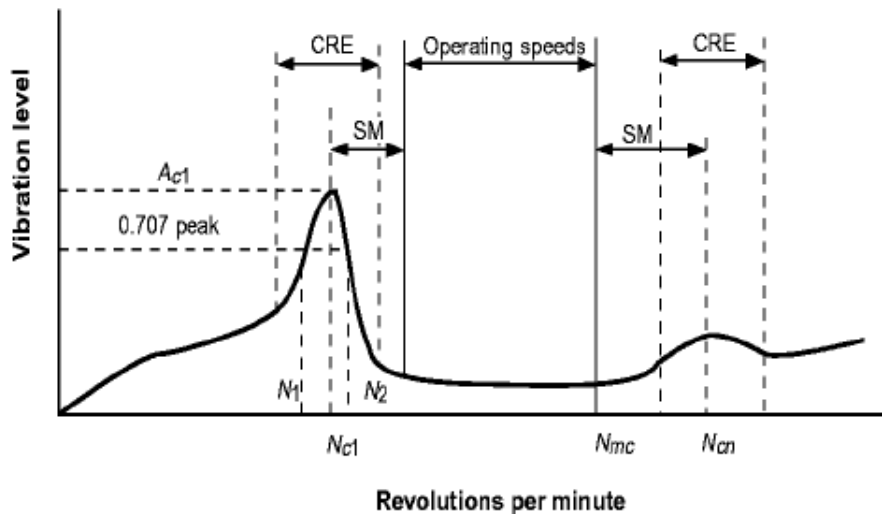
N_{c1} = Rotor first critical, center frequency, cycles per minute.
N_{cn} = Critical speed, nth.
N_{mc} = Maximum continuous speed, 105%.
N_1 = Initial (lesser) speed at $0.707 \times$ peak amplitude (critical).
N_2 = Final (greater) speed at $0.707 \times$ peak amplitude (critical).
$N_2 - N_1$ = Peak width at the half-power point.
AF = Amplification factor.

$$= \frac{N_{c1}}{N_2 - N_1}$$

SM = Separation margin.
CRE = Critical response envelope.
A_{c1} = Amplitude at N_{c1}.
A_{cn} = Amplitude at N_{cn}.

Figure 13. Synchronous amplification factor (AF) by half-power method (TPS)

An example of the change in AF due to changes in system damping is discussed below.   Figure 14 is a Bode plot from the shutdown of a reformer hydrogen recycle compressor in good condition. At some time later an event occurred and the overall vibration at running speed increased from approximately 1.0 to 3.0 mils pk-pk. The Bode plot from the subsequent shutdown is seen in Figure 15. As can be seen, the shape of the plot has changed considerably, the AF has increased substantially, and the first critical has dropped approximately 150 rpm. All of these changes indicate a reduction in stiffness and relative damping in the system. This particular compressor has floating ring oil seals, which do provide some damping as well, however it operates at relatively low pressures (approx.. 30 psig suction), so the seals are not a major contributor to the rotordynamics. Because of the change in AF, the compressor was shutdown at the next available opportunity and the bearings removed and inspected. As can be seen in Figure 16, the pads have indeed been damaged. The bearings were replaced and the compressor restarted. The recorded Bode plot is shown in Figure 17 and indicates that the AF has returned to its previous value.
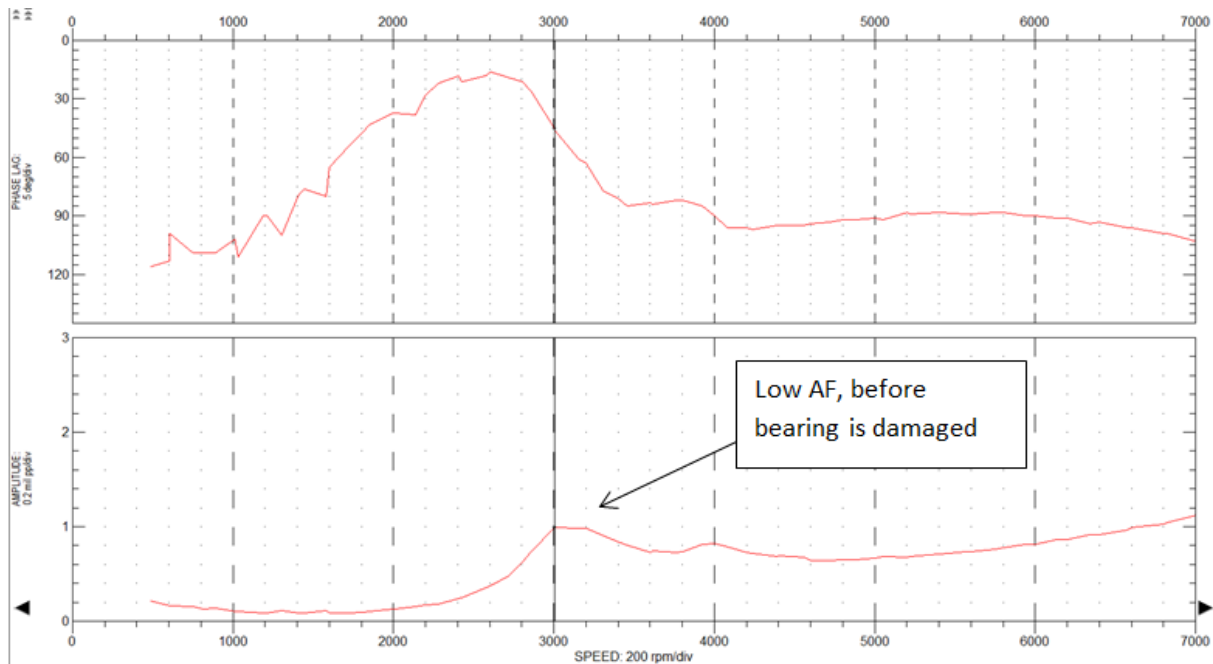
Figure 14. Bode plot from shutdown of reformer recycle hydrogen compressor (no issues)
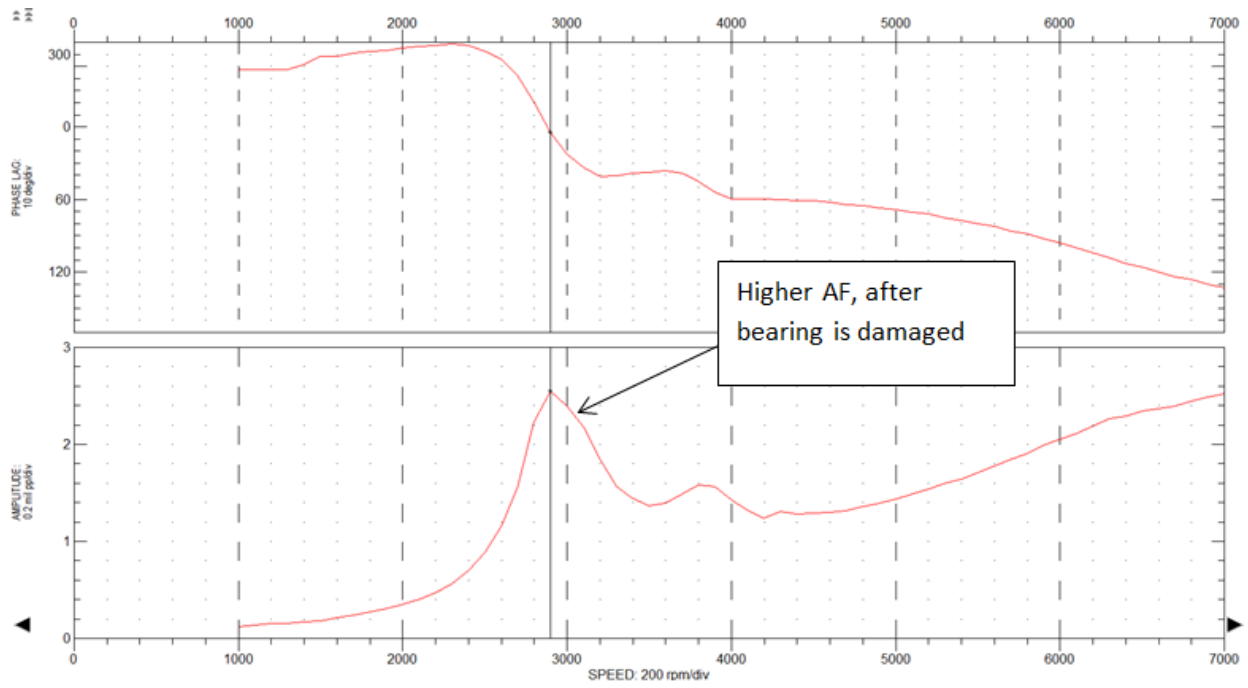
Figure 15. Bode plot from shutdown of reformer recycle hydrogen compressor, after event

Figure 16. Wiped tilt-pad bearing (due to insufficient lubrication) from reformer recycle hydrogen compressor
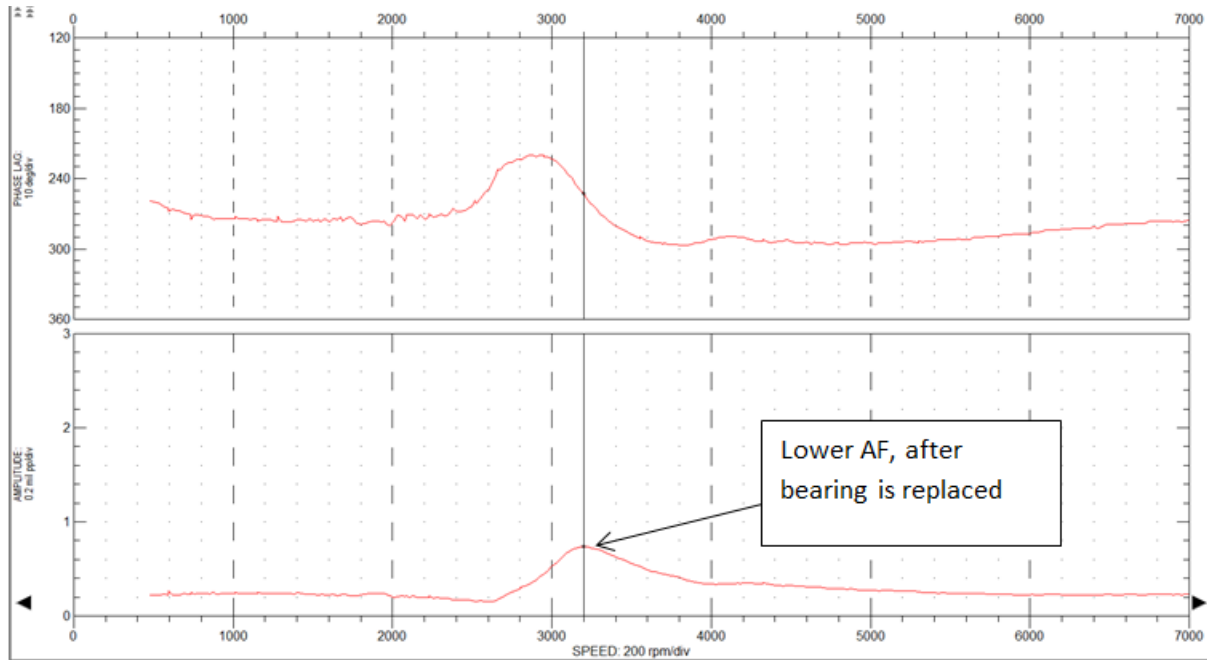
Figure 17. Subsequent start-up of reformer recycle hydrogen compressor after bearings were replaced.

An opposite example to the one above is another barrel compressor in the same refinery. A trend of the overall radial vibration from the drive end horizontal probe is shown below in Figure 18. As can be seen the radial vibration increased sometimes after a re-start. The overall level had increased from approximately 0.5 to over 4 mils in two years. A review of the mechanical shop test from the OEM, showed that the measured AF was approximately 4.5 when the compressor was new, see Figure 19.
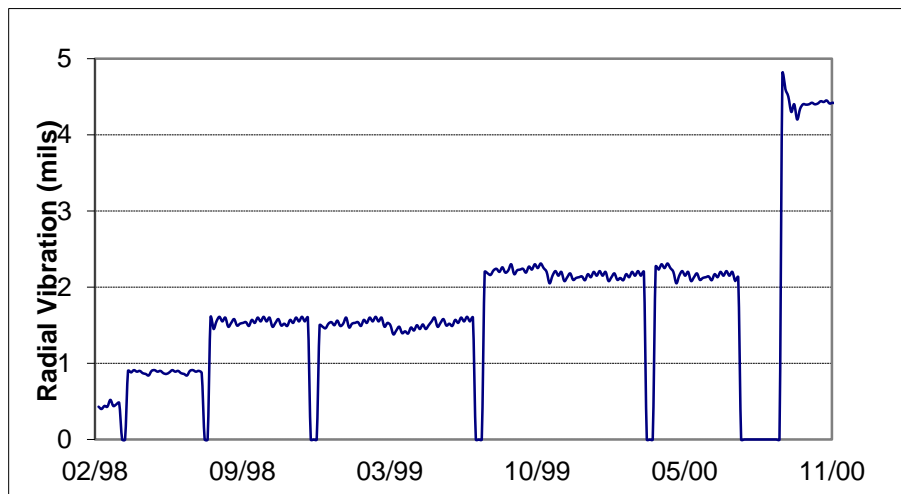
Figure 18. Trend of barrel compressor doverall vibration, drive-end horizontal for 2-3 year period
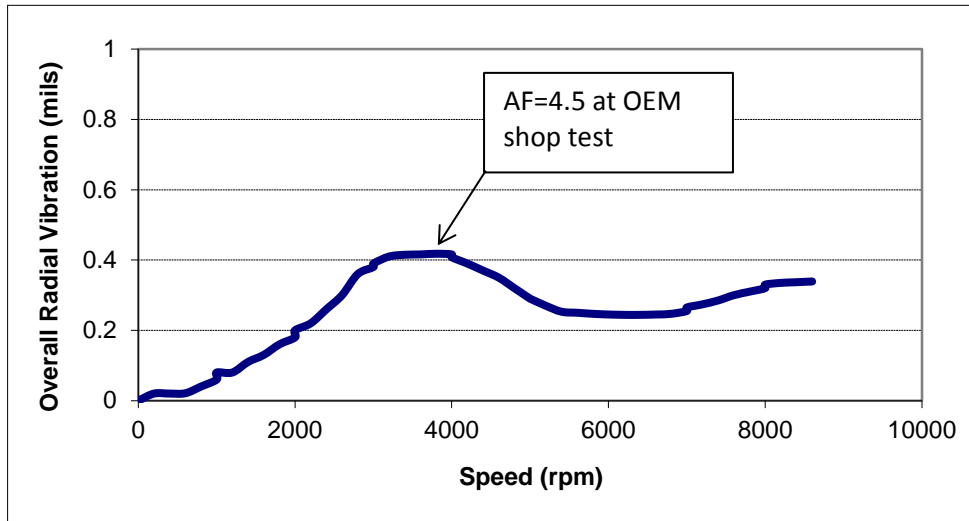
Figure 19. Overall vibration data from OEM shop test, compressor DE horizontal (AF=4.5)

Transient data was recorded during a start-up of the compressor which showed that while the vibration level was substantially higher, the amplification factor had not changed substantially, see Figure 20. Therefore, the increase in synchronous vibration was thought to have been the result of something other than bearing damage. This was not immediately obvious, since the increases in vibration shown in Figure 18 only occurred when the compressor was re-started, a common symptom of bearing damage from loss of lubrication. An extensive refinery wide shutdown approximately 9 months later resulted in the compressor being shutdown for one month. During the subsequent restart, the synchronous vibration had doubled to approximately 4 mils pk-pk; however, the measured amplification factor still remained relatively un-changed, see Figure 21. Likewise the slope of the phase change at resonance is very similar in both Figures 20 and 21. This further confirmed that the relative damping in the rotor system had not changed, indicating that the bearings had not been damaged. The compressor inner cartridge was pulled and found to be severely contaminated with porous media from the upstream process unit. The rotor was cleaned and re-installed with the same bearings and the maximum vibration levels at running speed returned to approximately 0.5 mils.
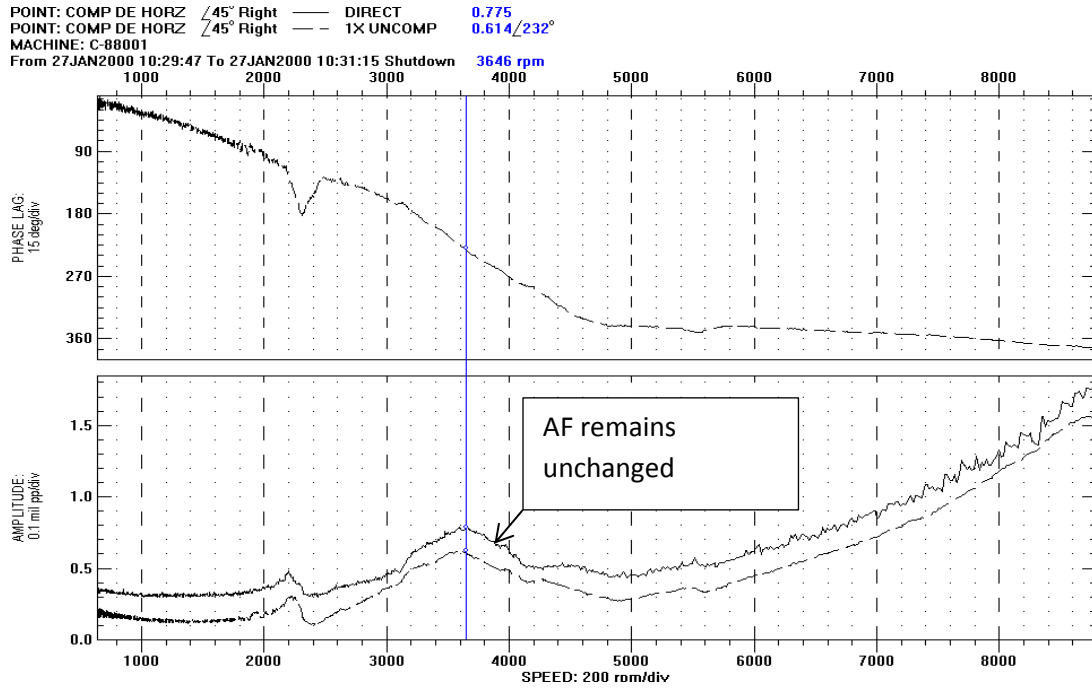
Figure 20 Barrel compressor drive end horizontal vibration, 01/2000 (AF =5.0)
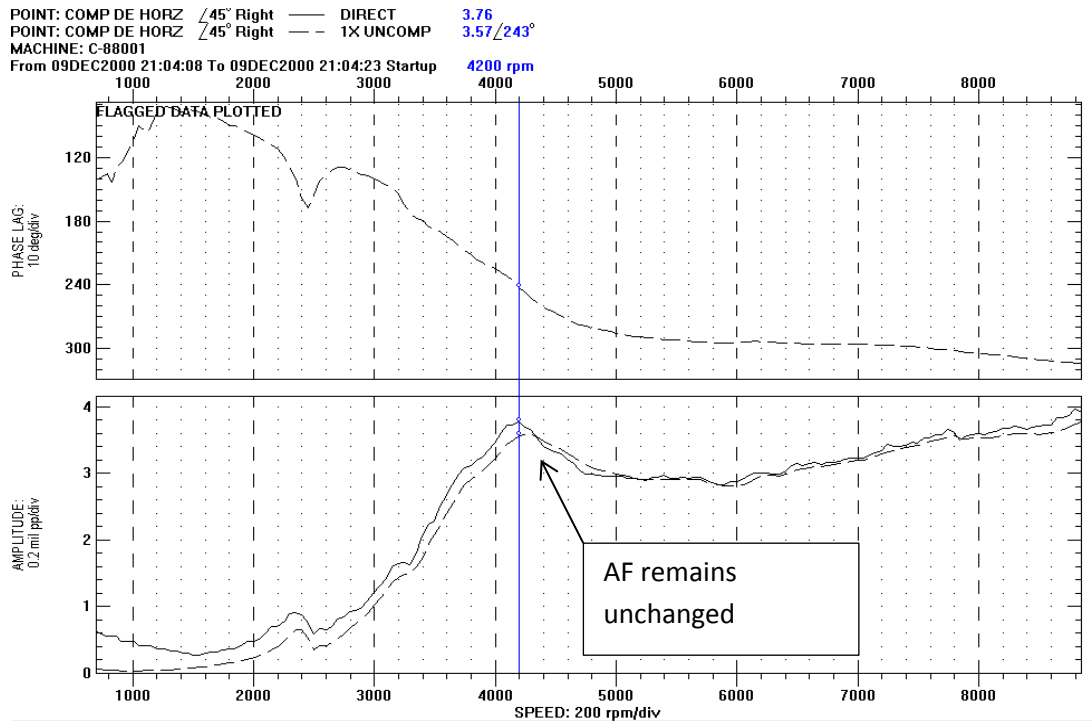

Figure 21 Barrel compressor drive end horizontal vibration, 12/2000 (AF =5.1)

As describe above, the ability to measure and predict natural frequencies in turbomachinery is extremely critical since most modern turbomachinery operates above at least one natural mode. This is obviously important, because when operating close to a resonance, the vibration can increase dramatically. Since the most common forcing function is the un-balance force, improved rotor balance many times has negligible benefits if operating close to a resonance. Typically, the best way to reduce vibration close to a resonance is to eliminate the resonance by moving the natural frequency. An example of this type of scenario occurred in an ethylene cracker unit in 2006. The unit had been shutdown for a 2 week turnaround to address some non-machinery issues. While the unit was down, an overspeed trip test was conducted on the steam turbine driver for the ethylene refrigeration compressor. The turbine's normal operating range was from 9,000-10,000 rpm; however, the maximum governor speed was 10,700 rpm. During the trip test the vibration on the turbine outboard increased dramatically above 10,000 rpm, see Figure 22. The vibration on the turbine prior to shutdown had been very low (approximately 0.5 mils), so the high vibration was certainly a surprise to the plant personnel. The second peak on Figure 22 along with the corresponding change in phase is an indicator of a resonance condition in the turbine. As a first step to investigate the problem, both radial bearings on the turbine were removed and the clearances checked. The clearance on the inboard bearing was within tolerance but the outboard bearing was 0.0005 in over the maximum. A rotordynamics model of the turbine was built to examine the problem further, see Figure 23.
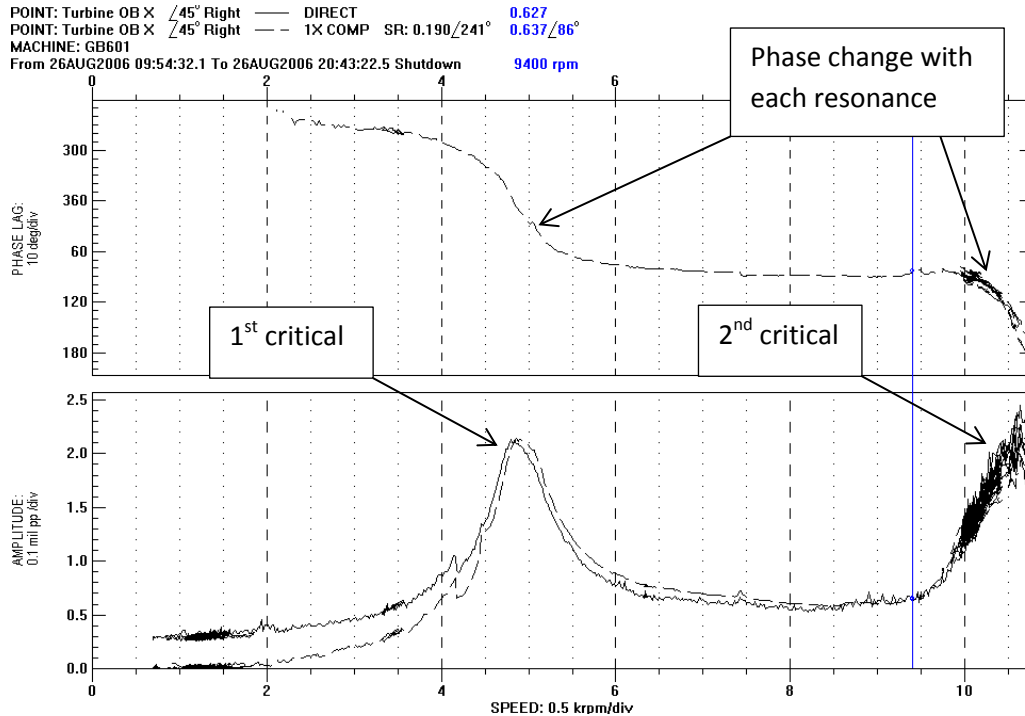

Figure 22. High speed steam turbine drive start-up, during over-speed trip test
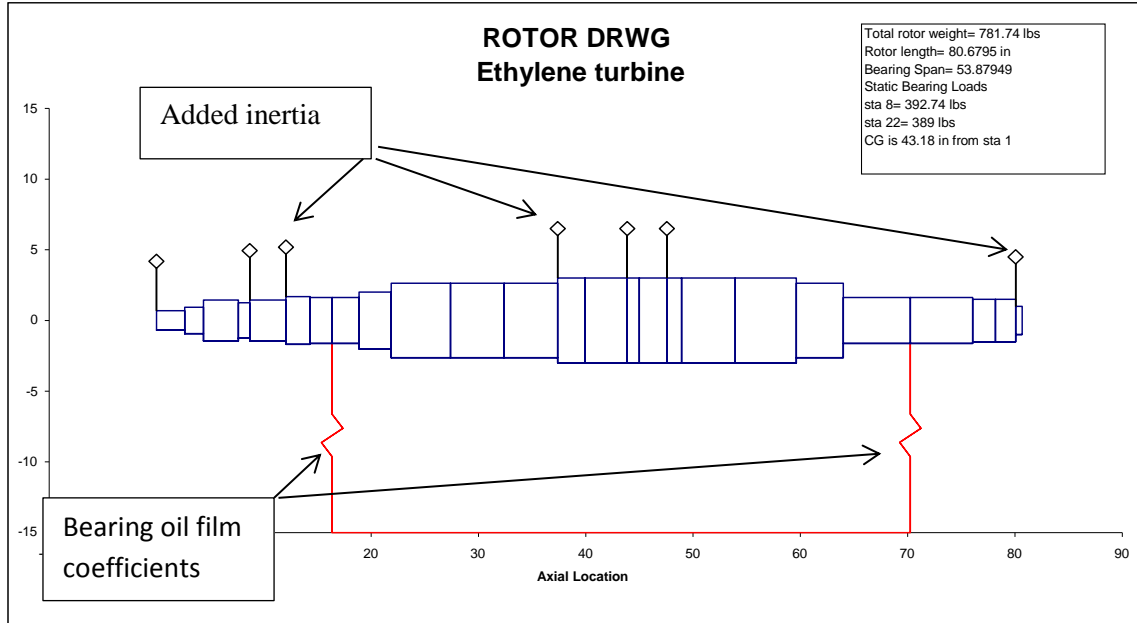
Figure 23. Graphical representation of ethylene turbine model with rigid bearing supports
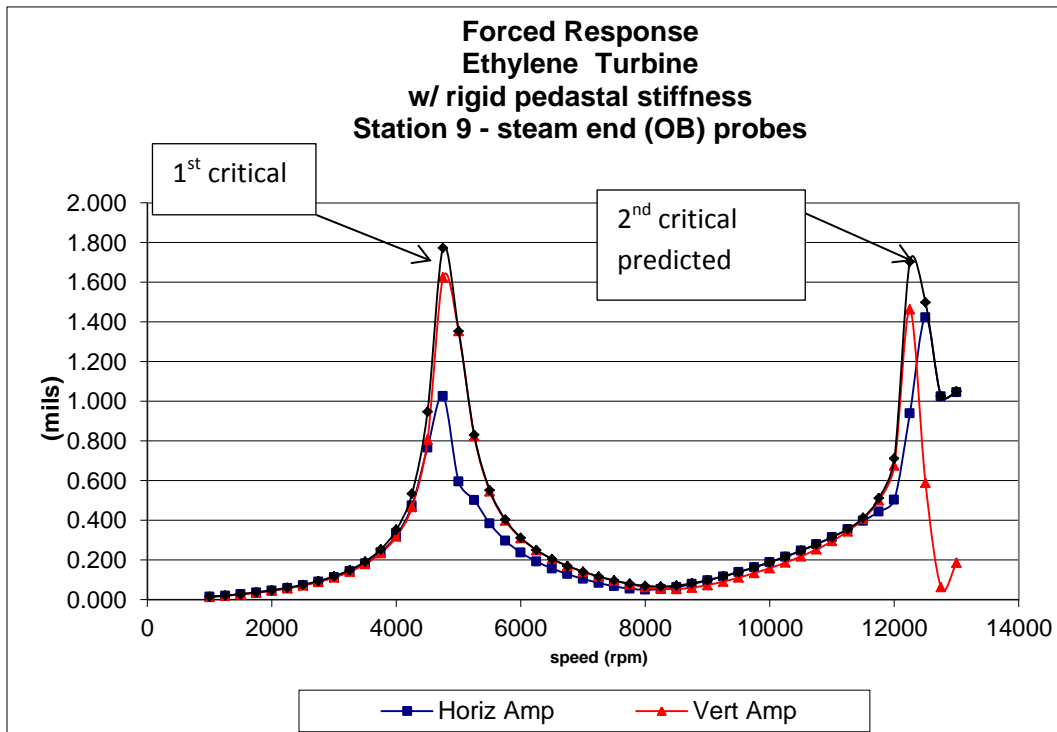

Figure 24. Ethylene turbine rotor model predictions w/o support stiffness effects (bearings on rigid supports)

The forced response calculations from the rotor model showed that the turbine's 2nd critical was approximately 12,200 rpm (see Figure 24), which was much higher than the value of 10,600 rpm shown in Figure 22. As is common on most steam turbines, the bearing support on the OB end is designed to be more flexible in the axial direction to allow for transient temperature gradients during start-up, see Figure 25 . Sometimes this can result in a lower radial stiffness as well. To "tune" the rotor model to the actual vibration, the outboard end bearing housing support stiffness was calculated and added to the rotor model, see Figure 26. A detailed explanation of this is covered in Ref[7]. The resultant forced response calculations reflected were much closer to the actual vibration response, see Figure 27. To address the problem the plant personnel installed a radial bearing that was actually 0.0005 in under the minimum design range of the bearing (the pads were shimmed to reduce the clearance). The Bode plot of the resulting start-up of the turbine after the outboard bearing modification is shown in Figure 28. The lower bearing clearance had increased the system support stiffness enough to move the 2nd critical above the turbine's operating speed range.

OB flexible support
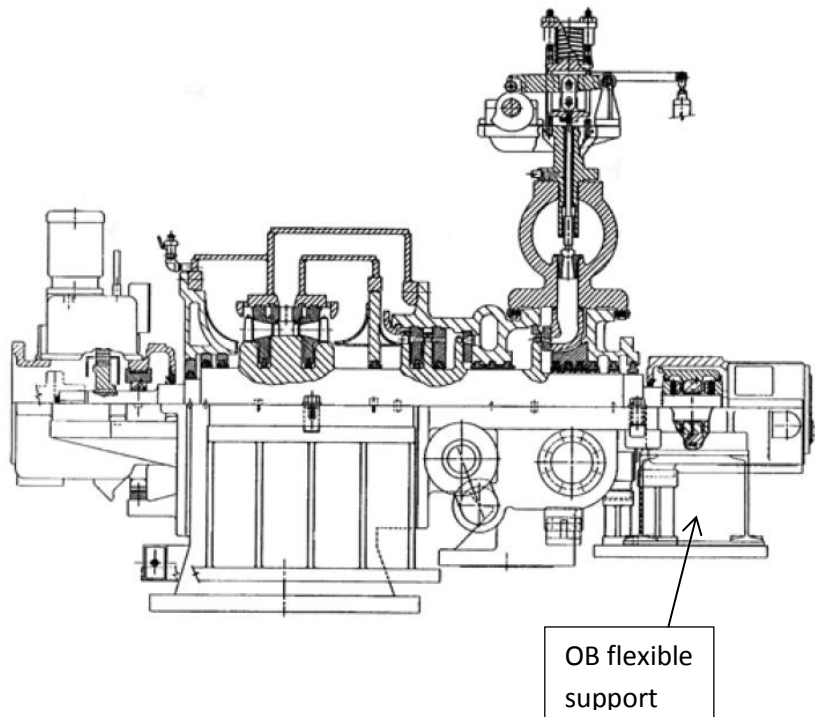
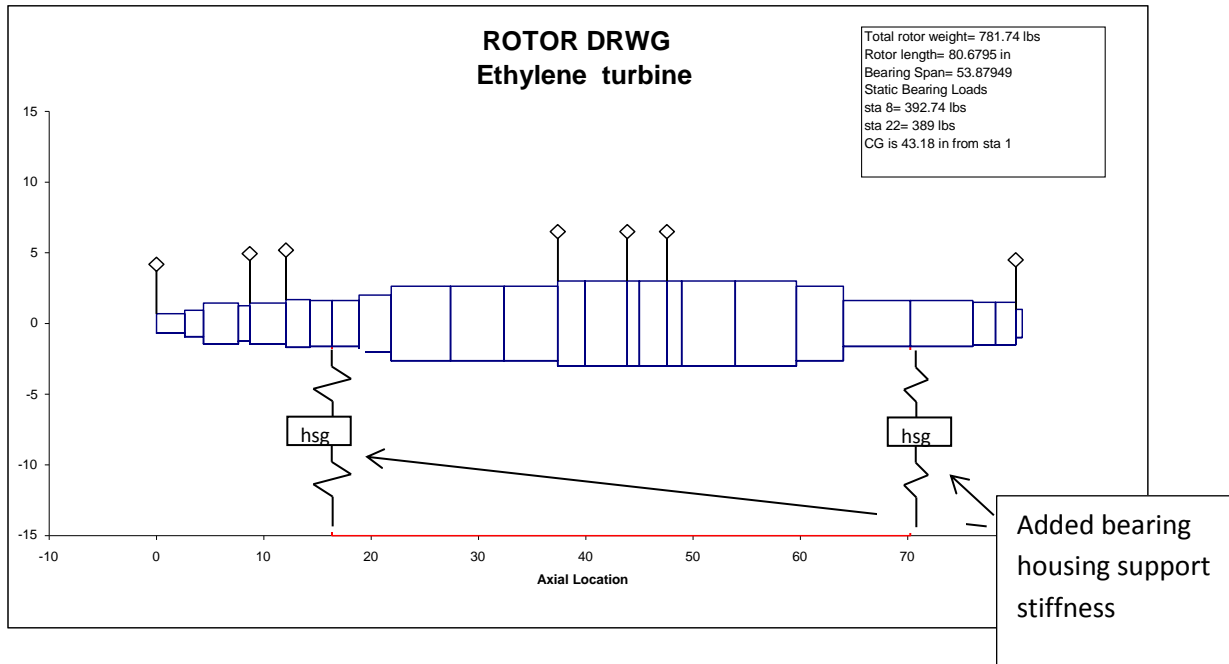*Figure 25. Typical mechanical drive steam turbine cross-section (TPS)*

Figure 26. Graphical representation of ethylene turbine model with bearings on flexible supports
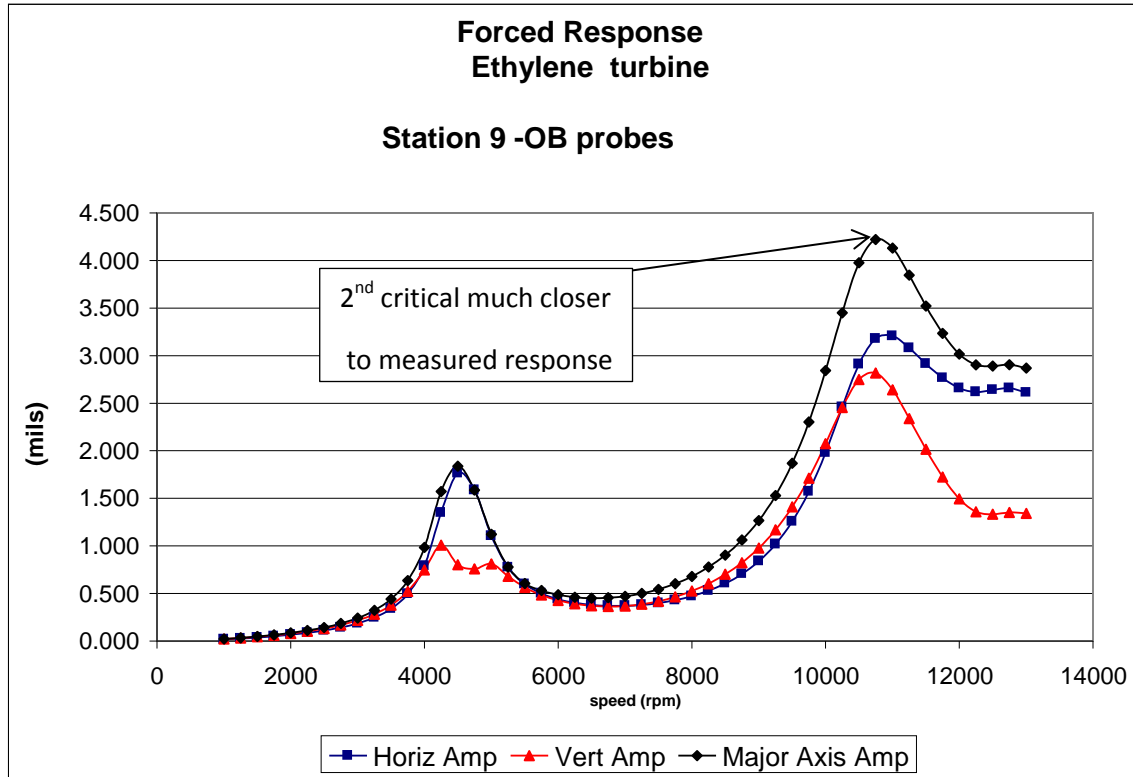
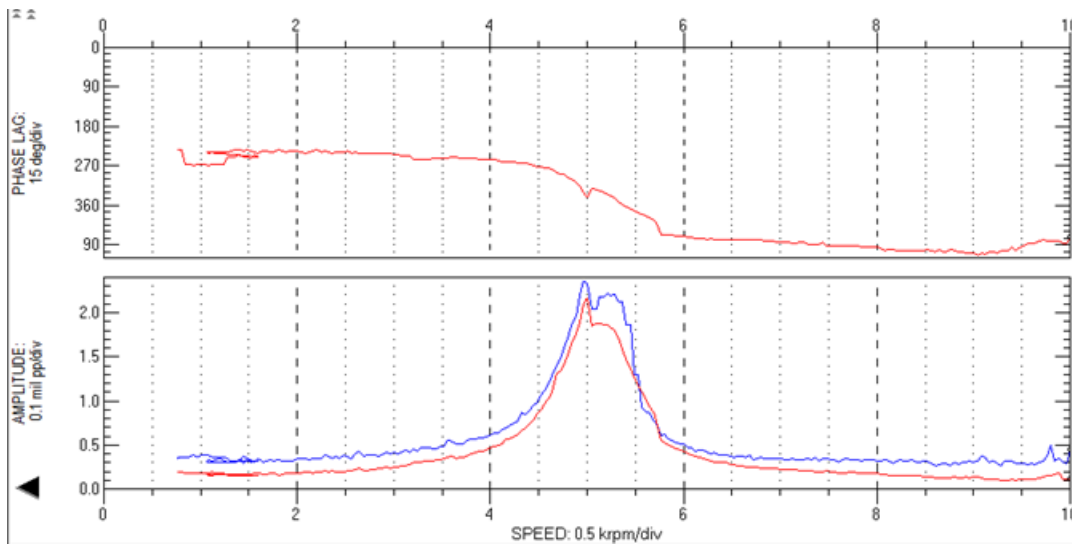*Figure 27. Ethylene turbine rotor model predictions w/ support stiffness effects (bearings on flexible supports)*

Figure 28. Steam turbine bode plot after outboard bearing was replaced (reduced clearance)

Cascade and Waterfall Plots

The cascade and waterfall plots are actually multiple FFT spectrums that are plotted versus speed (cascade) or time (waterfall). Both plots are excellent for identifying non-synchronous vibration issues that occur during transient conditions.   One disadvantage of the cascade and waterfall plots is the data acquisition time(DAT) required for the FFT, which is defined by:

$$DAT = \frac{NL}{F_{max}}$$

where NL= the number of lines in the spectrum and F_{max} is the maximum frequency in the spectrum. The DAT is the minimum time required to acquire the number of samples for each spectrum. This is important because if the speed of the machine in question is changing very rapidly, then some data maybe lost during the acquisition time. As an alternative, most analyzers have the ability to acquire multiple vector samples (i.e. 1x, 2x, etc) between spectrums, this allows for much more rapid vector data acquisition during transient events.

An example of using advanced vibration analysis to troubleshoot multiple problems on a propylene export compressor is described below. The compressor is a horizontally split design that operates at 9800 rpm and contains 5 impellers in a single section. It compresses propylene from approximately 30 to 280 psig. After an inspection overhaul, the start-up vibration on the compressor had increased dramatically in comparison to the values at shutdown. The synchronous amplitude was high but steady; however, the sub-synchronous component at 37% of running speed was very erratic, see Figure 29. The sub-synchronous frequency of 3600 cpm was very close to the compressor's measured first critical speed. This all pointed to an excitation frequency close to the first critical, however, the waterfall plot shown in Figure 30 shows that the subsynchronous component did not appear until the compressor was almost up to full speed. This particular compressor has 5 pad, LBP bearings, and dry gas seals which eliminates oil whirl as a potential excitation. Likewise, oil whirl would typically begin tracking once the rotor speed was 2X the rotors 1st critical (i.e. about 7000 rpm). Troubleshooting the compressor revealed that the sub-synchronous component was very dependent on discharge pressure, see Figure 31. This also coincided with why the sub-synchronous vibration didn't appear until the compressor was up to full speed.
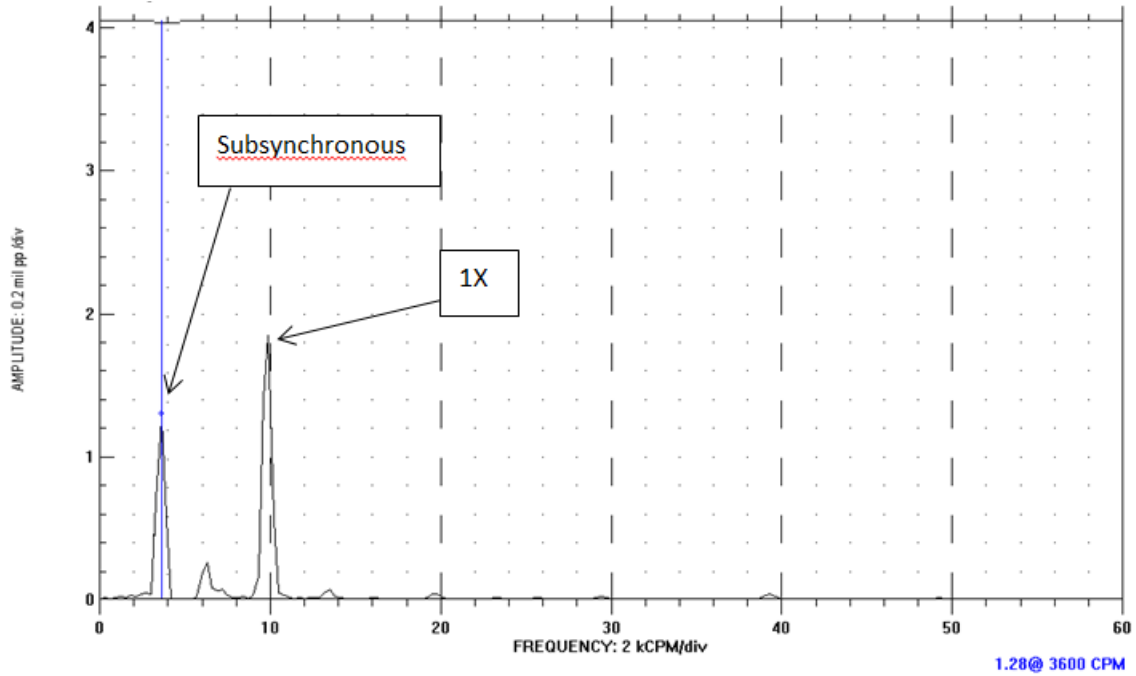
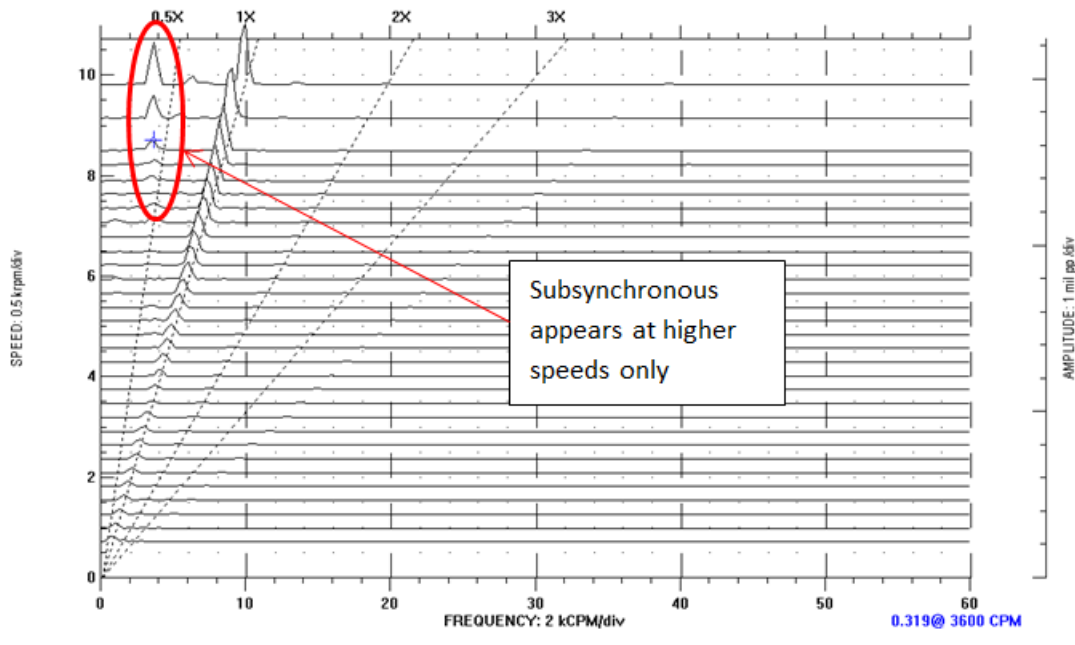*Figure 29. Compressor drive end vertical spectrum after overhaul*

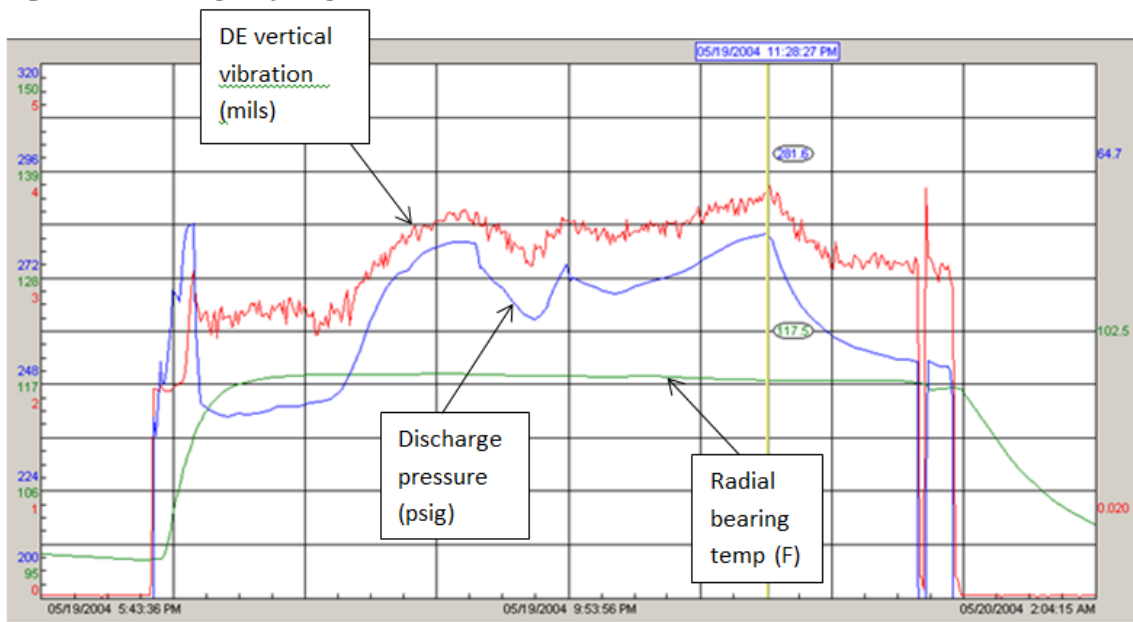*Figure 30. Cascade plot of compressor drive-end vertical*

Figure 31. Trend showing discharge pressure(blue), drive end radial bearing temperature(green), and overall drive end horizontal vibration(red)

A rotordynamic study was conducted to help determine the cause of the high sub-synchronous vibration. For a compressor of this pressure level, the aerodynamic effects of the impellers and interstage labyrinth seals are normally not that significant. The largest destabilizing forces are normally contributed by the balance drum seal for a compressor of this caliber and this machine was no exception. The balance drum seal on this machine incorporated a rotating labyrinth versus an abradable stationary, see Figure 32. An illustration of the rotor model is shown in Figure 33 and the calculated 1st eigenvector w/o aerodynamic effects is shown in Figure 34. The balance drum seal was added to the rotor model and the log decrement of the 1st mode for a range of discharge pressure was calculated, see Figure 35. This stability map strongly supported the correlation between vibration and discharge pressure shown in Figure 30 above. Additionally, the original reason for the overhaul was to inspect the abradable stationary on the balance drum seal. Several failures of the abradable stationary seal due to thermal expansion had occurred in the previous ten years see Figure 36. During the most recent overhaul, the end gap clearance on the seal was increased to prevent these types of failures. Reviewing the previous inspection records and failure analysis after the vibration problem determined that the end gap may have been increased too much, causing excessive leakage through the balance drum seal. This was supported by the rotor's axial position after the overhaul, which indicated that the rotor was running on the inactive or "discharge" side. All indications pointed to the cross-coupled stiffness produced by the balance drum seal as the source of the destabilizing forces which excited the rotor's 1st mode.
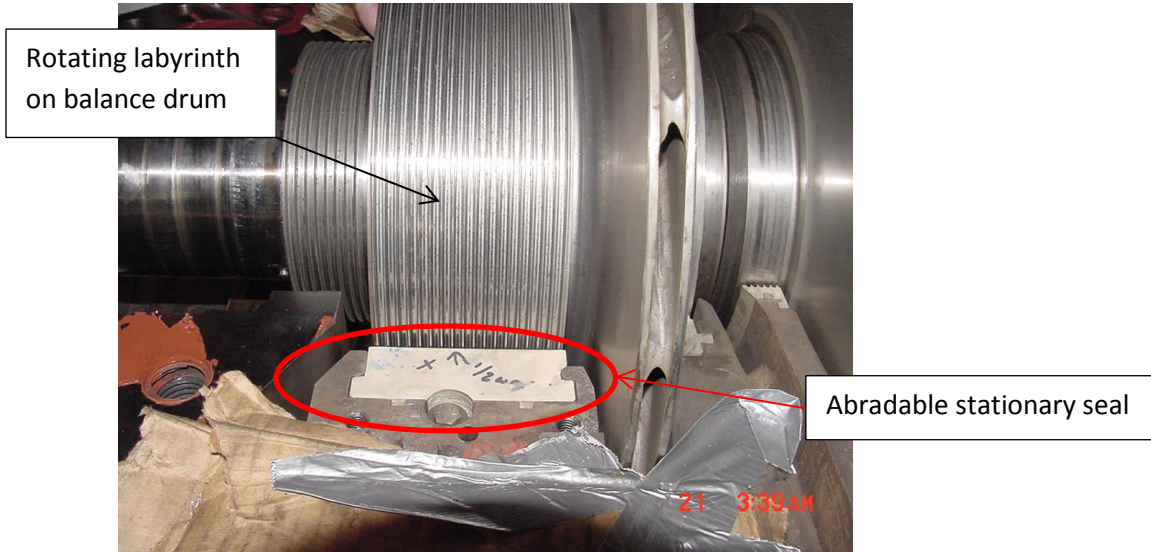
Figure 32. Rotating labyrinth seal on balance drum with abradable stationary

SHAFT DRWG

Total rotor weight= 897.18 lbs
Rotor length= 80.239 in
Static Bearing Loads
sta 10= 445.44 lbs
sta 56= 451.74 lbs
CG is 41.59 in from sta 1

bearing

bearing

Labyrinth seals

Balance
drum seal

Axial Location

Figure 33.   Illustration of propylene compressor rotor model
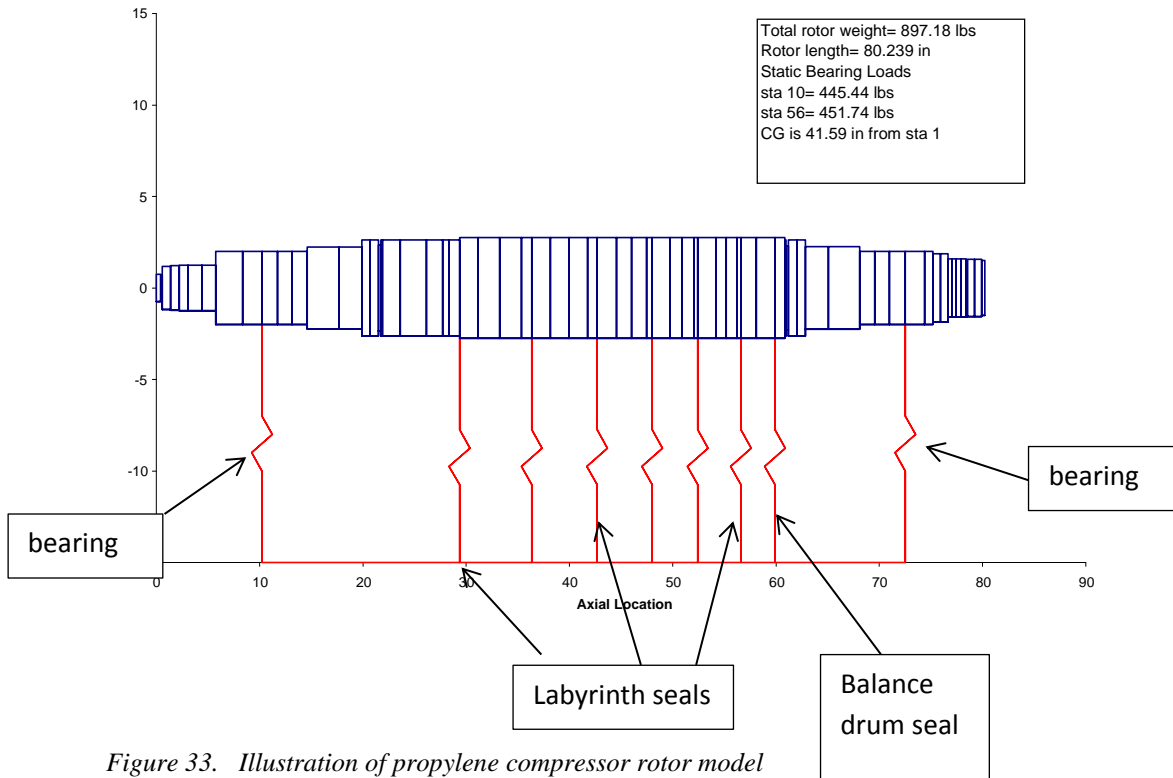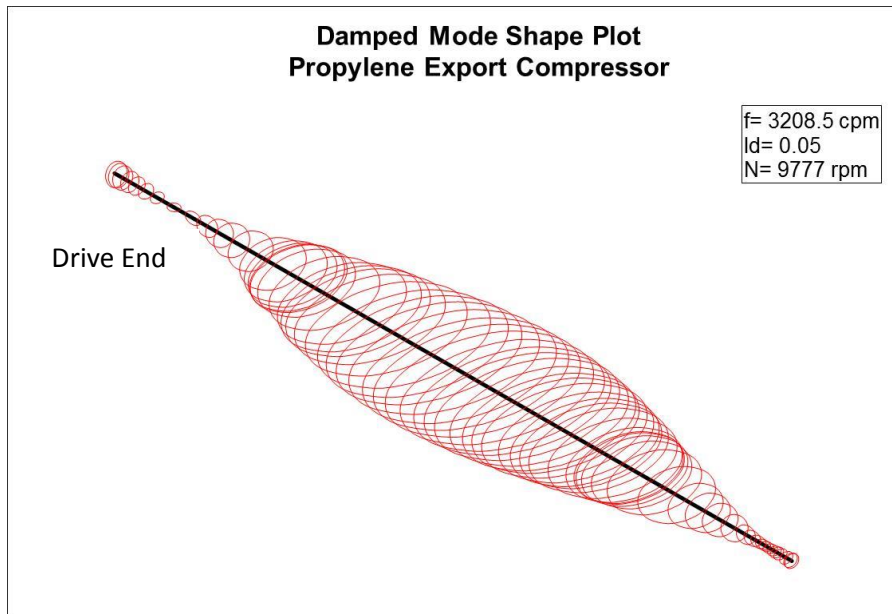
Figure 34. Calculated 1st mode for propylene export compressor with original bearing (5 pad, LBP, Cd=0.005, m=0.35, L/D=0.36), w/o aerodynamic effectsof balance drum seal
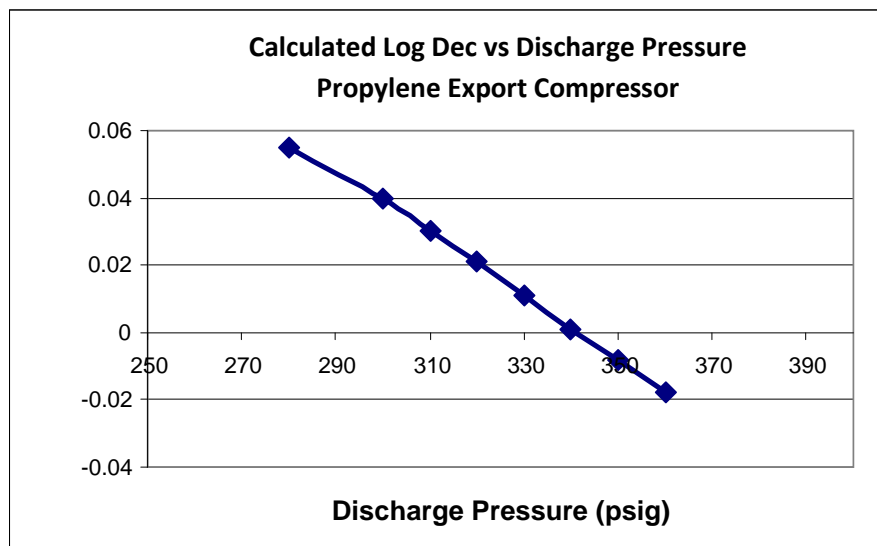
Figure 35. Calculated stability as function of discharge pressure with original bearing (5 pad, LBP, Cd=0.005, m=0.35, L/D=0.3)
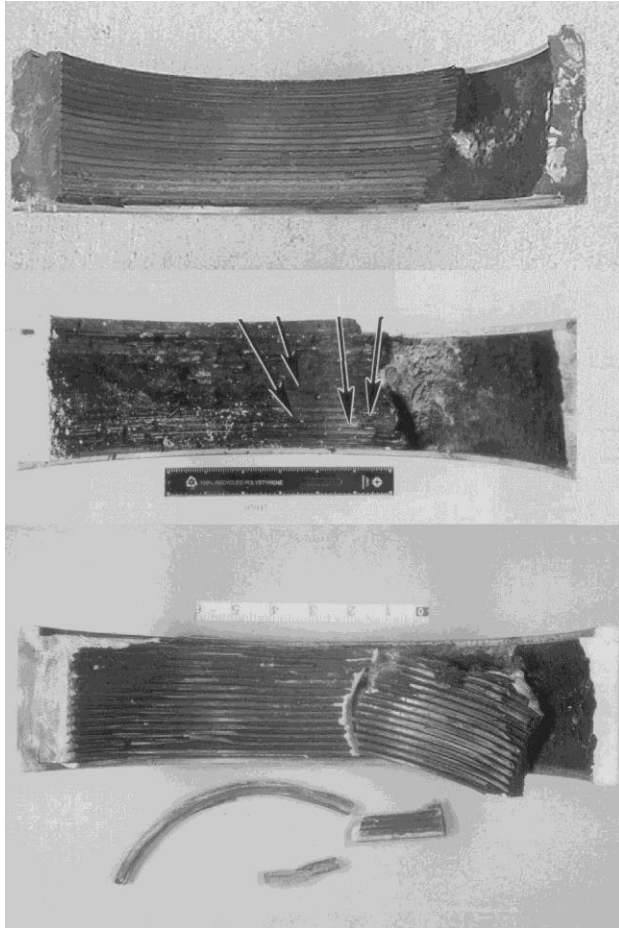
Figure 36. Failed abradable balance drum seals from 2001(upper), 1997(mid), and 1994 (lower)

The most direct method to address the problem would be to reduce the cross-coupled stiffness produced in the balance drum seal. An alternative design with swirl brakes on the inlet was designed and fabricated. However, replacement of the balance drum seal would have required a substantial outage and the vibration was kept somewhat under control by limiting the compressor discharge pressure.

As an immediate stop-gap type repair, an improved tilt-pad bearing was designed that changed the bearing design from a LBP to a LOP, increased the L/D, and lowered the pre-load slightly. A more detailed background of the methodology of these changes can be found in Ref[8,9]. These design changes increased the effective damping in the bearing and improved the calculated log decrement from 0.05 to 0.2, see Figure 37. To confirm the stability predictions, during an at-speed balance check of the spare rotor, the transient data was recorded with the original and the optimized bearing designs. As can be seen in Figures 38 and 39 the amplification factor is significantly higher with the original bearing design design in comparison to the optimized. The optimized bearing was installed during a short outage and the overall vibraiton was reduced from approximately 1.9 to 0.4 mils, see Figure 40.
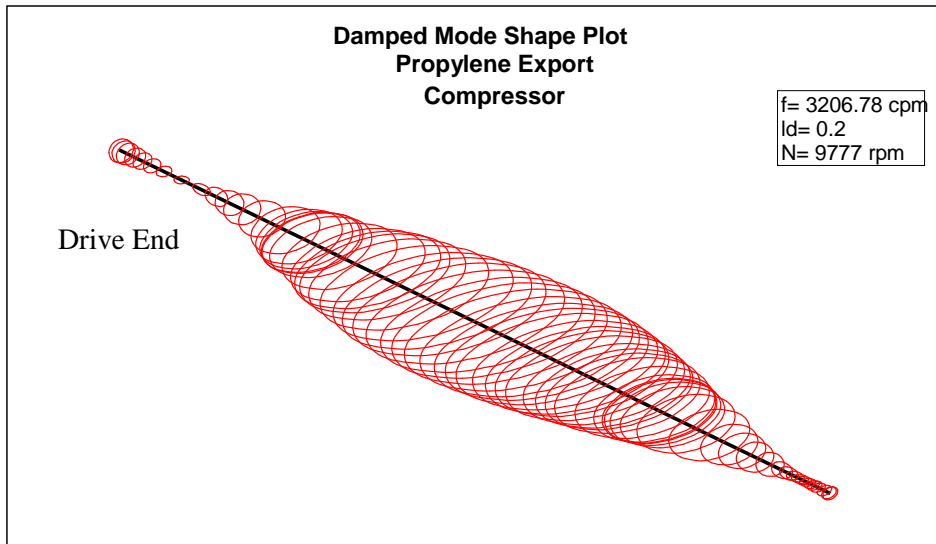
Figure 37. Calculated 1st mode with modified bearings (5 pad, LOP, Cd=0.006, m=0.2, L/D=0.4) and 360 psig discharge pressure
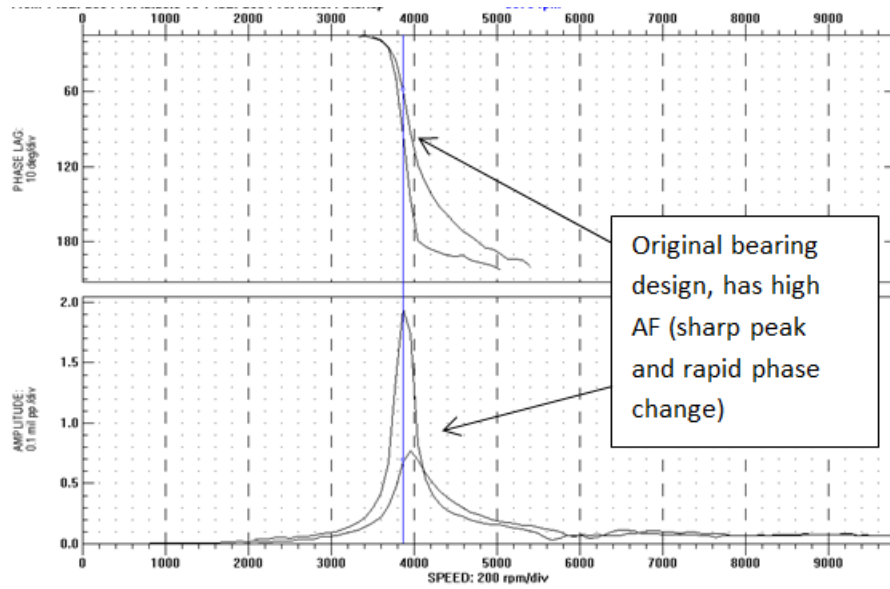
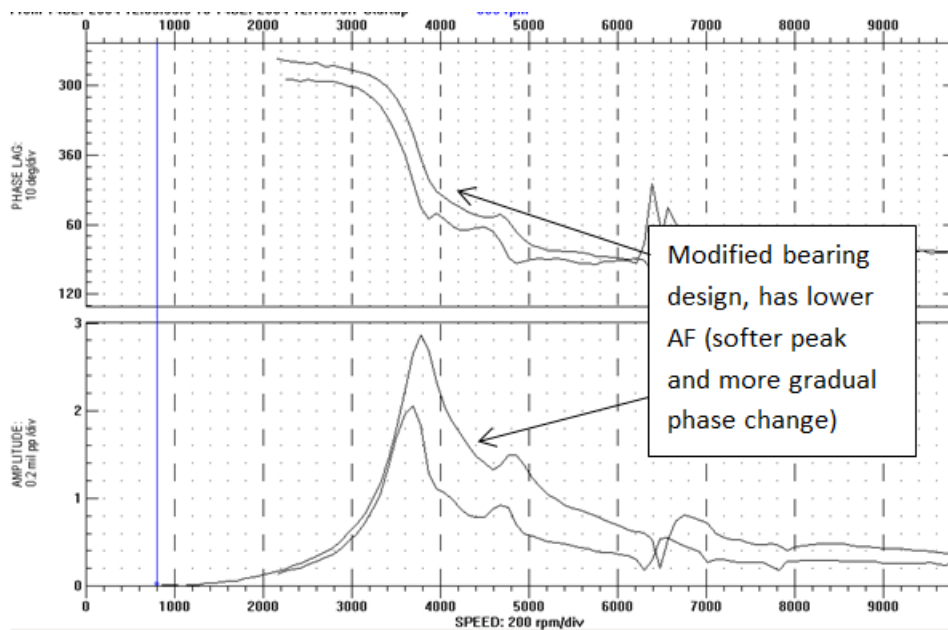*Figure 38. Rotor response with original LBP bearing, Cd=0.005, L/D=0.3, m=0.495*

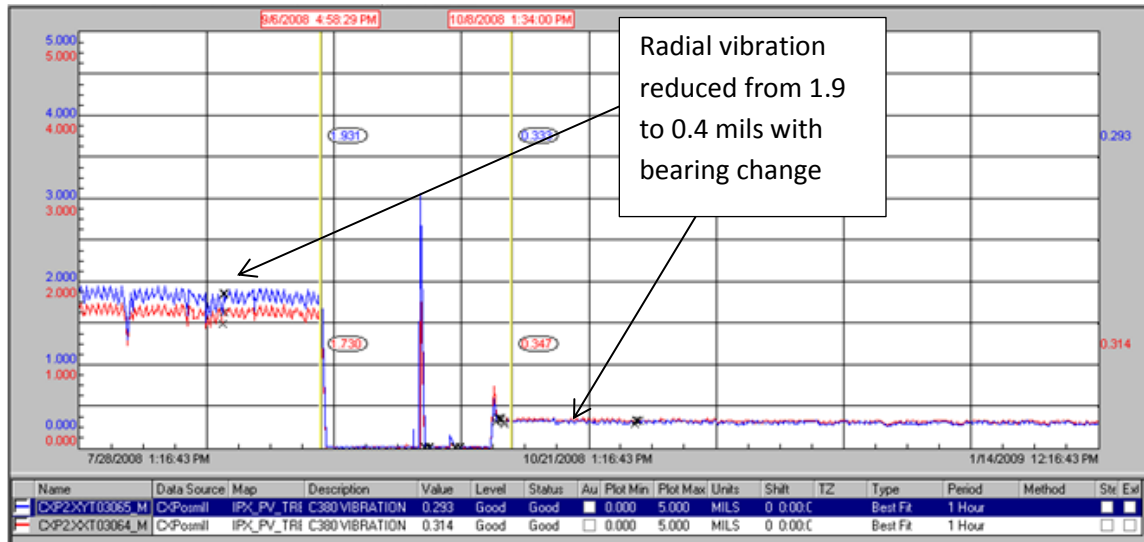*Figure 39. Rotor in ASB bunker with optimized LOP bearing, Cd=0.006, L/D=0.4, m=0.2*

Figure 40. Trend of propylene compressor drive end vibration before and after bearing change

As discussed above, the proximity of a rotor's speed to a natural mode can have a dramatic effect on the produced vibration. The frequency of the rotor's natural modes must be well known and the corresponding mode shapes understood. An example of <u>not</u> understanding the deflected mode shape is revealed when a refinery FCC wet gas compressor experienced an increase in vibration, see Figure 41. The compressor was a two section design with oil seals and was relatively old, see Figure 42. The increase in vibration was thought to have been caused by foulant falling off the compressor rotor while it was down. The largest increase in vibration was on the non-drive (thrust) end of the compressor. Since this was also the 1st section of the compressor (rhs of Figure 42), it was assumed that a solvent wash in the inlet of the compressor might improve the vibration. Repeated attempts to "clean" the rotor on-line were un-successful. The compressor was operated a short while longer until a maintenance outage could be scheduled. Inspection of the compressor internals revealed that fouling was not the cause of the high vibration. The front cover on the 5th stage wheel (1st impeller in the 2nd section) had failed at the rivet, see Figure 43 which resulted in a substantial unbalance. Even though the 5th stage impeller was closer to the drive end of the compressor, the radial vibration had been substantially higher on the non-drive end because of the displaced mode shape of the rotor at operating speed. The amount of missing impeller cover was measured and the unbalance effect was calculated to be approximately 20 oz-in. The calculated displacement at both drive end and non-drive end probes due to the estimated unbalance on impeller #5 is shown in Figures 44 and 45. As can be seen the predicted values on the non-drive end are substantially higher even though the unbalance is quite far away from those probes.

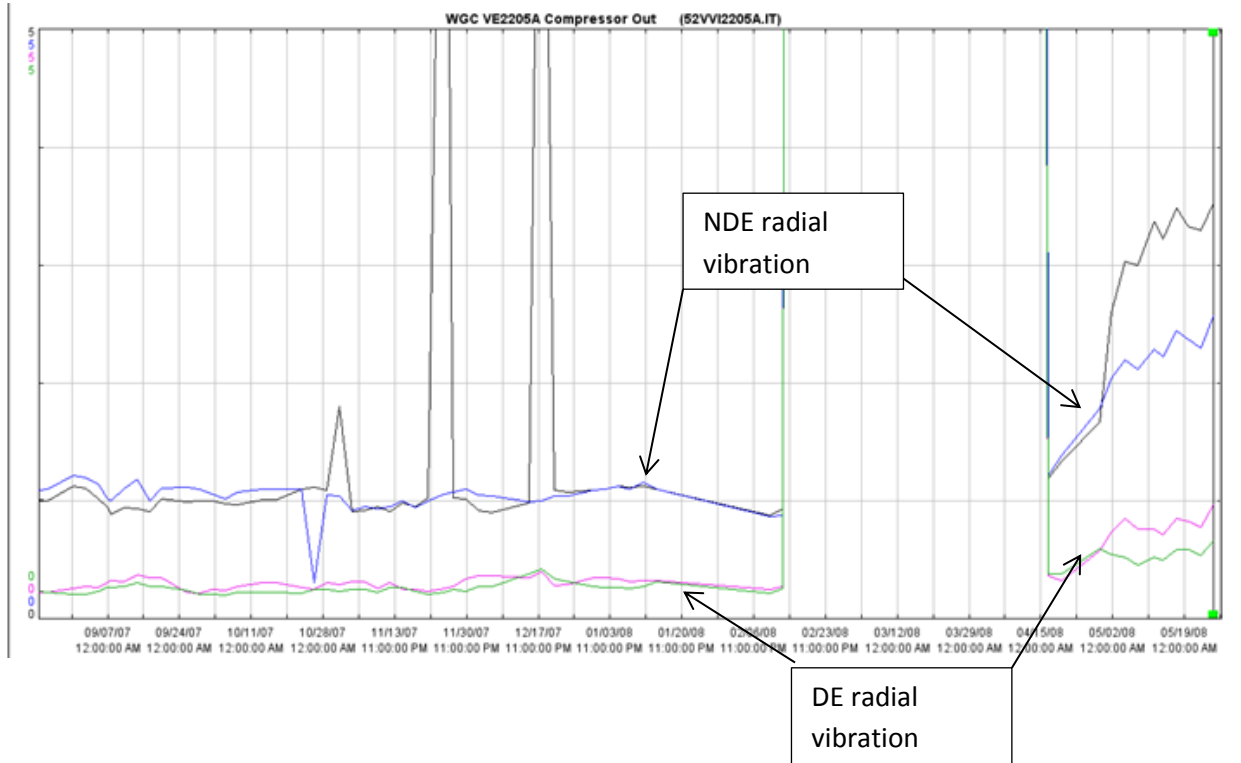*Figure 41. Trend of FCC wet gas compressor overall radial vibration before and after unit outage (blue/black NDE, green/pink DE)*
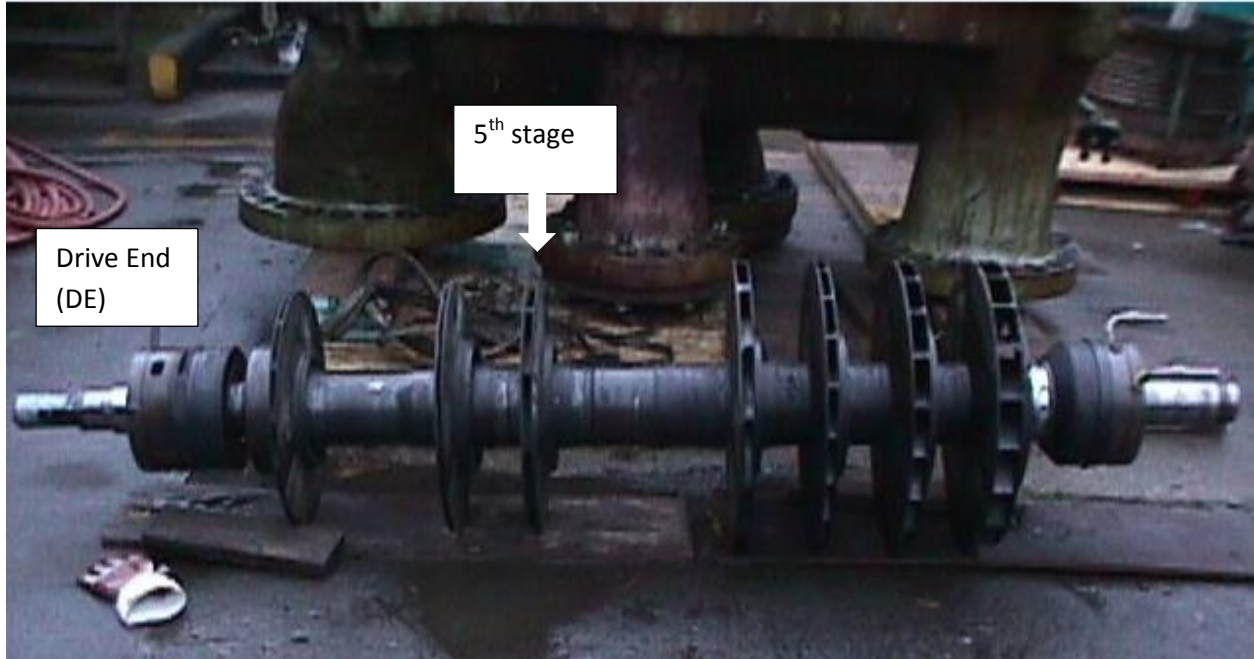
5th stage

Drive End (DE)

Figure 42. FCC wet gas compressor rotor during previous overahaul

rivets

Figure 43. FCC wet gas compressor failed 5th stage impeller, note rivets

Forced Response
FCC Wet Gas Compressor
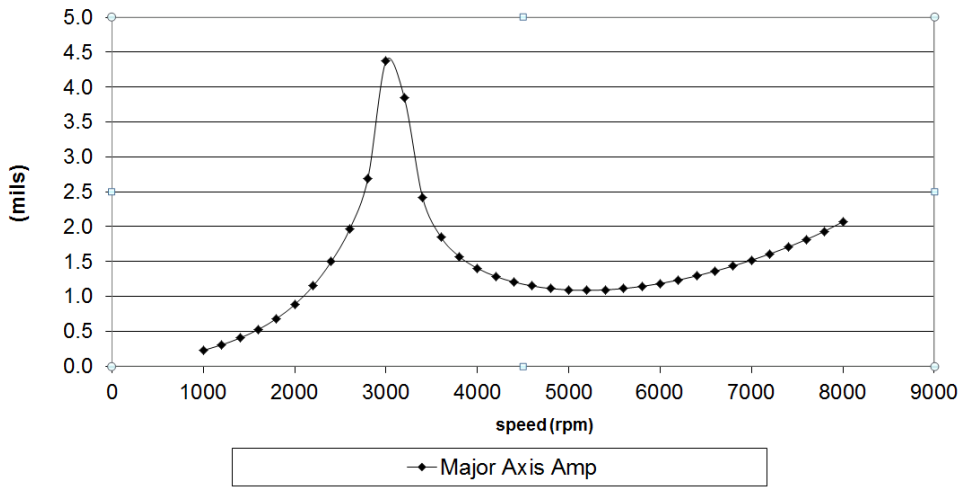**20 oz-in unbalance at 5th stage impeller**
Station 7 - DE probes

Figure 44. FCC wet gas compressor forced response calculations on drive end probes for calculated unbalance

Forced Response
FCC Wet Gas Compressor
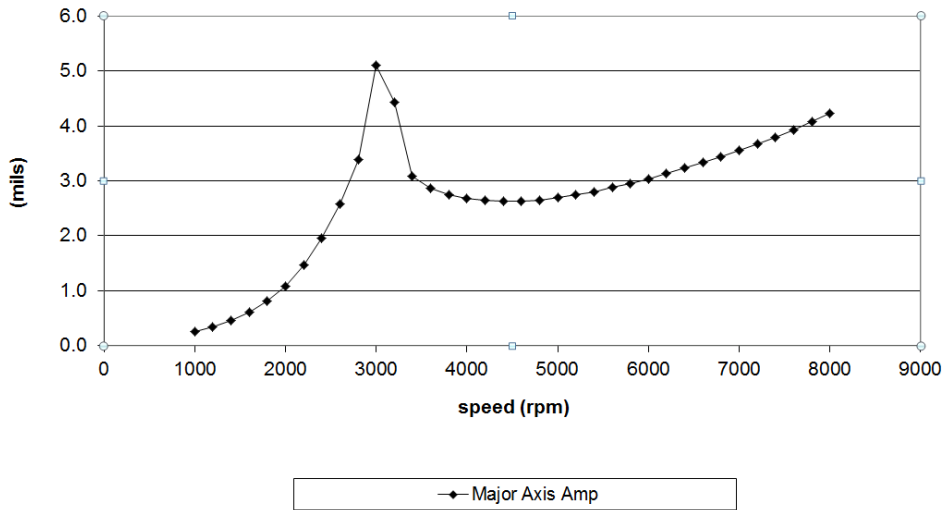**20 oz-in unbalance at 5th stage impeller**
Station 34 - TE probes

Figure 45. FCC wet gas compressor forced response calculations on non-drive end probes for calculated unbalance

SHAFT CENTERLINE AND ORBIT PLOTS

Two vibration diagnostic plots that are only available for proximity probes are the shaft centerline and orbit plots. As described above the proximity probe system produces both a DC and AC signal. If two orthogonal probes are used, the signals from these two probes can be combined to provide significant insight into the machine behavior. The DC signal represents the average shaft position from the proximity probe tip. The most common application is when the shaft speed is changing (typically start-up and shutdown). Since the shaft rides on a film of oil, it rises up from the bottom of the bearing as the speed increases. A typical shaft centerline plot for the start-up of a centrifugal compressor is shown in Figure 46. The characteristic of this plot is very dependent on the individual machine type, bearing design, and application. Shaft centerline plots are very good for determining if the rotor is obstructed by a stationary component or if the bearing clearance is out of tolerance (either too low or high). Likewise, trends of shaft position over time can be used to determine if a bearing has been damaged, allowing the rotor to drop down in the bearings. The shaft orbit plot is created by plotting the time waveform (i.e. AC components) of two orthogonal probes versus each other, which represents the whirling motion of the shaft inside the bearing. A separate illustration of how the shaft orbit is produced from two proximity probe signals is shown in Figure 47. Additionally, an illustration of the shaft centerline and orbit plots is shown in Figure 48.
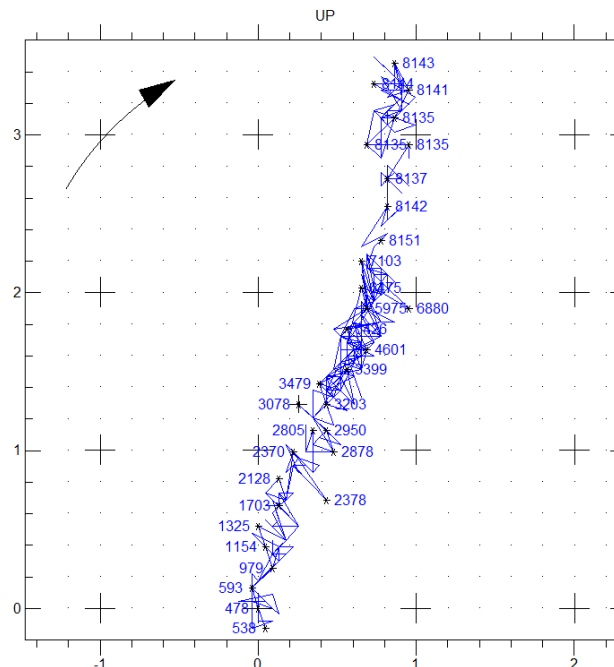

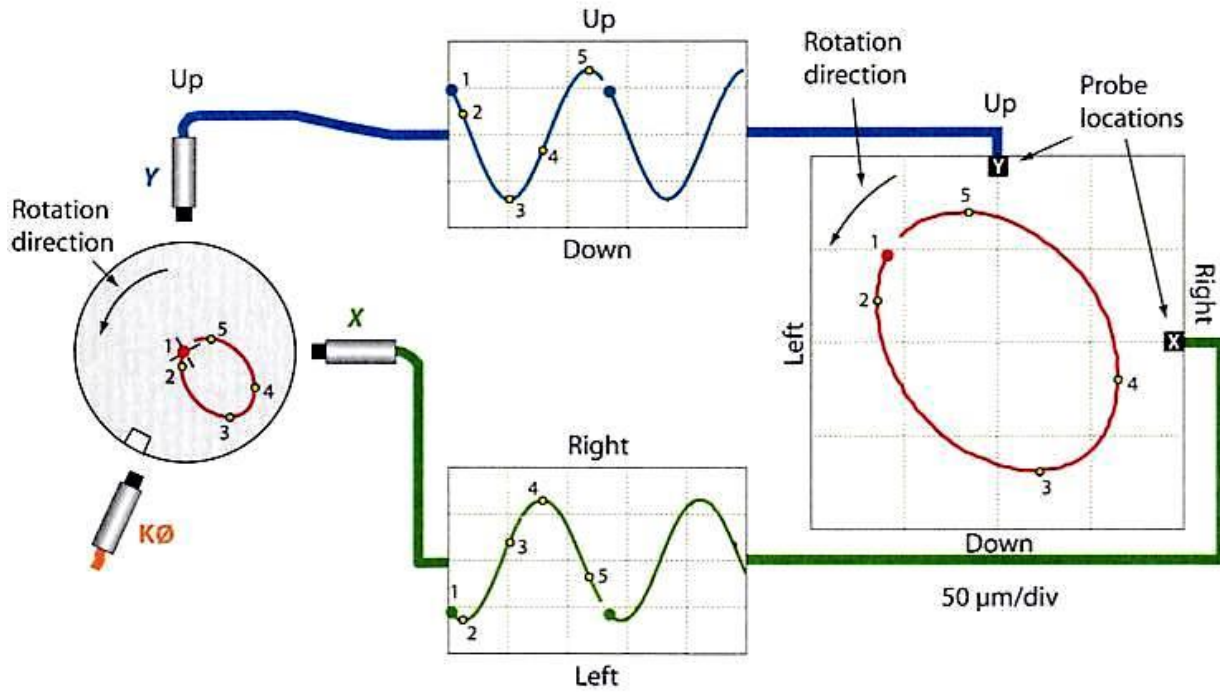*Figure 46. Typical shaft centerline plot of a start-up of a centrifugal compressor on tilt-pad bearings*

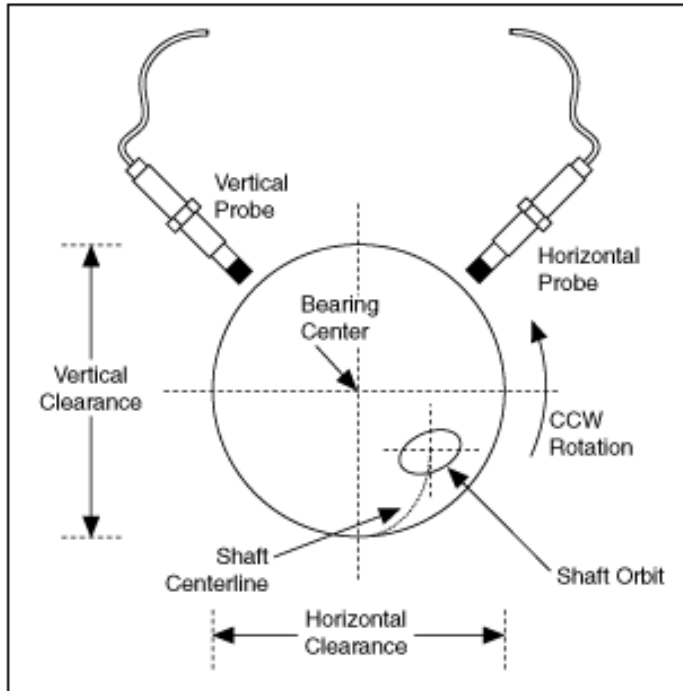*Figure 47. Relationship between time waveforms and shaft orbit (General Electric)*

Figure 48. Illustration of shaft centerline and shaft orbit plots (General Electric)

A good example of the utilization of both shaft centerline and orbit plots is an industrial gas turbine generator exhibiting higher than normal vibration after a major inspection. The #2 and #3 bearings had been replaced, along with the blades on all three turbine stages. The initial thoughts were that there was a balance problem since the blade arrangement is very critical and nearly all of the vibration was synchronous. However, comparison of the shaft centerline plots of a previous start-up and the most recent showed a marked change.   While the previous start-up (Figure 49) is very typical of a machine on tilt-pad bearings, Figure 50 shows that a rub of some type occurs sometime above 2340 rpm. This causes the rotor to be pushed back down as the speed in increased. This can be observed in the orbit plots as well. Figures 51 and 52 show higher amounts of pre-load on the rotor, which causes the orbit to become more elliptical/distorted. A short inspection of the #3 bearing after the overhaul revealed that the rub/preload may have damaged one of the pads in the #3 bearing, see Figure 53.
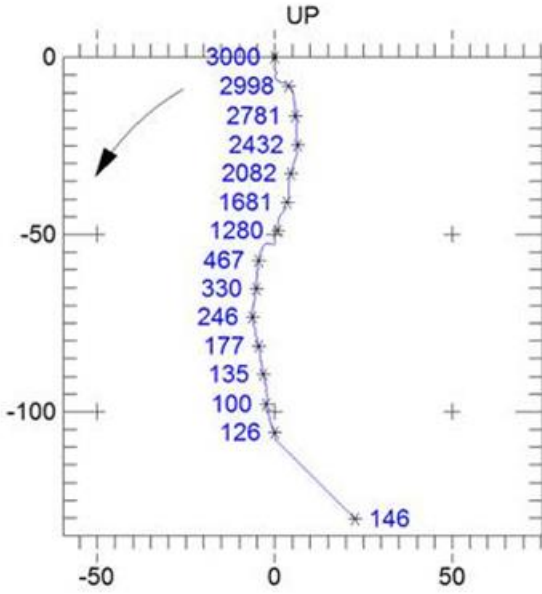
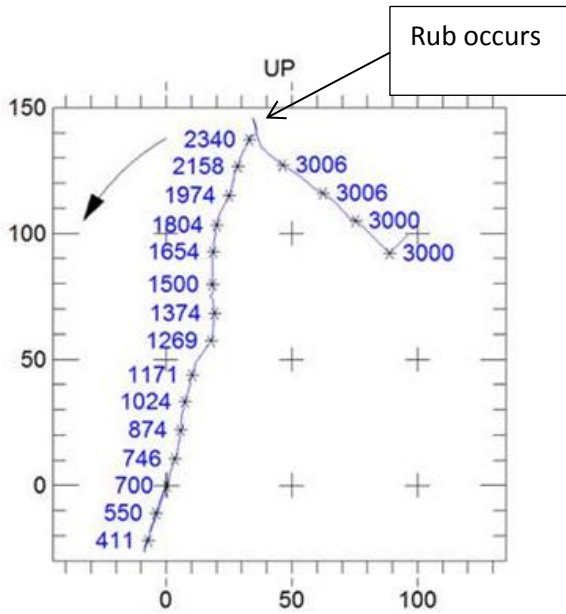*Figure 49. Turbine bearing #3 shaft centerline plot, before major overhaul*

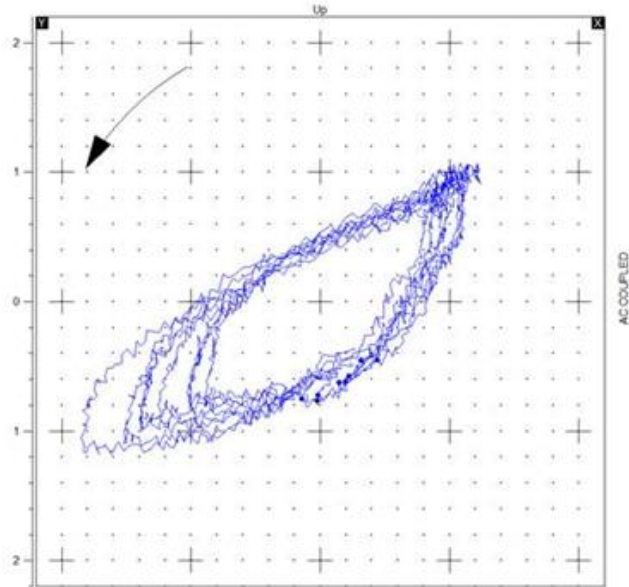*Figure 50. Turbine bearing #3 shaft centerline plot, after major overhaul*

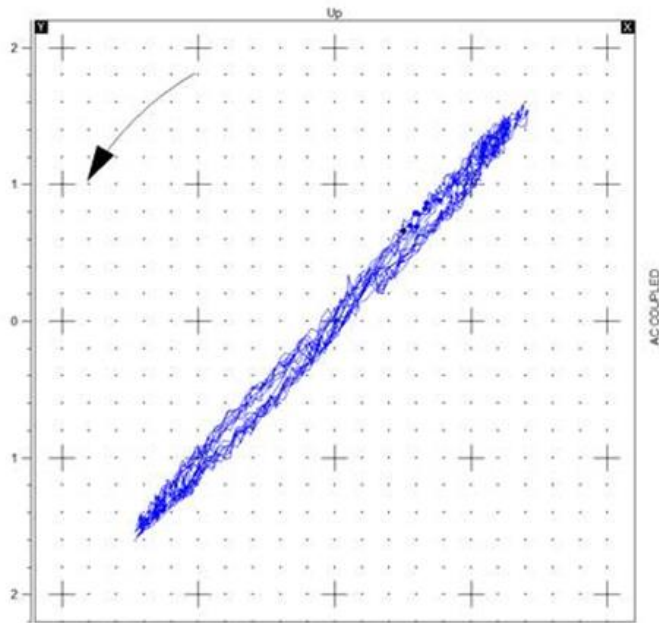*Figure 51. Turbine #3 bearing shaft orbit with preload after overhaul*

Figure 52. Turbine #3 bearing shaft orbit showing extreme preload after overhaul

Figure 53. Damaged pad from #3 bearing found during bearing inspection after overhaul

Another example of using a cascade, bode, orbit, and shaft centerline plots to troubleshoot machinery issues centers around a 30 MW gas turbine generator. The application is a two-shaft aeroderivative gas turbine that drives a 4-pole electrical generator through a parallel shaft reduction gearbox, see schematic in Figure 54. During a FAT, a very high (approximately 12 mils) radial vibration was observed on the pinion drive end (DE) bearing, see Figure 55. This only occurred during a tripped breaker test at full load (i.e. the breaker on the generator was opened when the generator was operating at full load). This is normally performed to test the package controls ability to trip in a rapid fashion and prevent a rotor overspeed event. The very high vibration occurred during coastdown and only for a narrow speed range. Initial concern was that this was a torsional resonance, being excited during the transient event.   However, the OEM measured the torsional vibration on both the bull gear and pinion shafts and the amplitudes were all low. Likewise, there was no component at the 41 hz shown below in Figure 56. Examination of the shaft centerline plots during the test led to the final solution. The generator load was increased and decreased multiple times during the FAT, this change in power resulted in corresponding changes in radial gear load, which are represented by the multiple lines up and down in Figure 57. The gear radial load is a direct function of the power being transmitted and acts along the gear load angle, which is approximately 20 degrees from vertical. This radial gear load pushes down on the bull gear and up on the pinion, see Figure 58. The relatively high radial gear

load keeps the pinion very stable in the top half of the pinion bearings when power is being transmitted. To handle low power (and subsequent low gear load) situations, the gearbox was designed with a pressure dam in the lower half of the pinion bearings. Normally, this pressure dam creates an upward radial load on the pinion to keep it stable when the gear load is not sufficient. During the open-breaker test, the gear load was dramatically reduced. Likewise, for a short period of time, the inertia of the large four pole generator acted as a flywheel to prevent the relatively light power turbine rotor from slowing down, see Figure 59. This inertial breaking affect, reversed the transmitted radial load within the gearset, which tried to lift the bull gear and pull the pinion down. The transient reverse gear load is not enough to lift the bull gear, but it is enough to cause the pinion shaft to become unstable and whirl, causing the very high vibration shown in Figure 55. The pressure dam bearing design was changed by increasing the dam width and changing the dam location from 45 degrees off bottom dead center to only 15 degrees. This change not only increased the load produced by the dam, but changed the load angle so that it was more in-line with the gear load at 20 degrees. The subsequent open breaker trip of the generator after the bearing design changes, showed that the shaft centerline plot had changed and the high vibration had been eliminated, see Figures 60, 61, and 62. The high vibration on the extreme left of Figure 61 was caused by the jacking oil pumps being started on the generator at 100 rpm and being transmitted through the gear mesh. Since the shaft speed was so low, the energy is very low andit is not a concern other than the vibration trip that may occur.
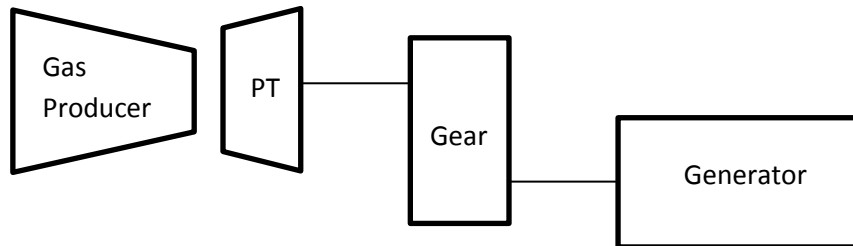

Figure 54. Schematic of two shaft gas turbine generator with speed reducing gearbox
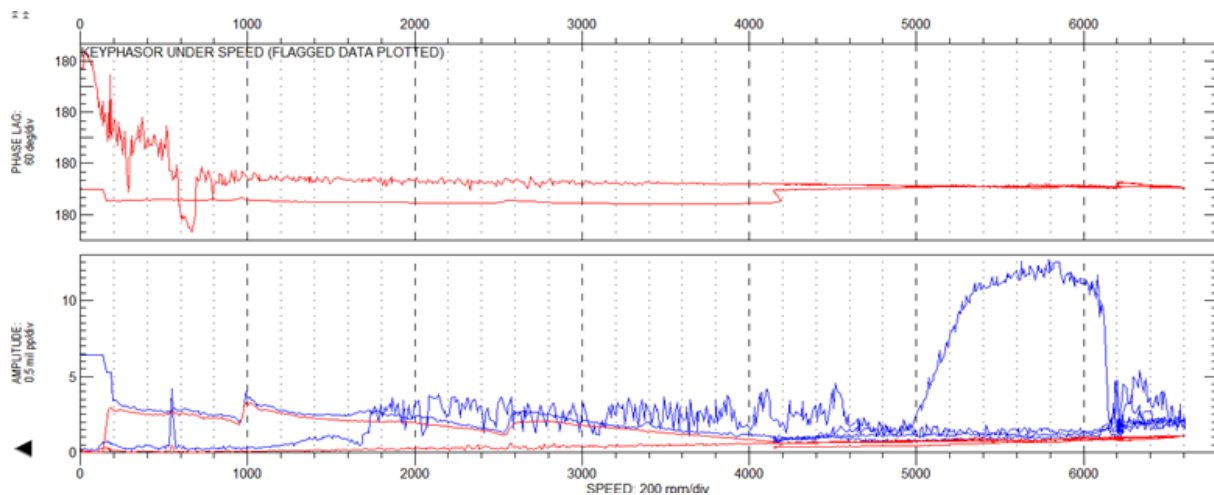

Figure 55. Bode plot of gearbox pinion radial overall (blue) and 1x(red) vibration on gas turbine generator
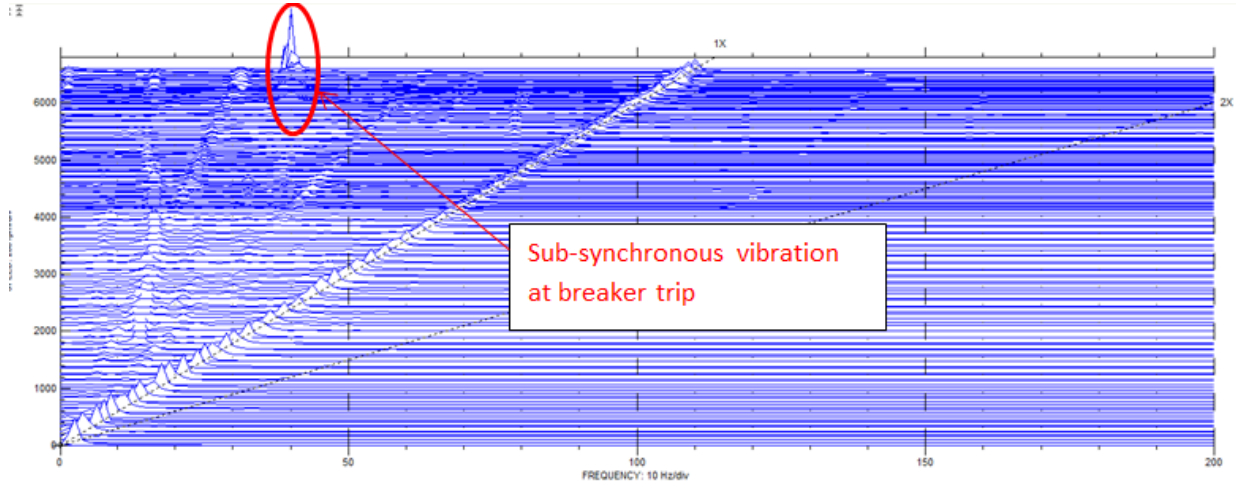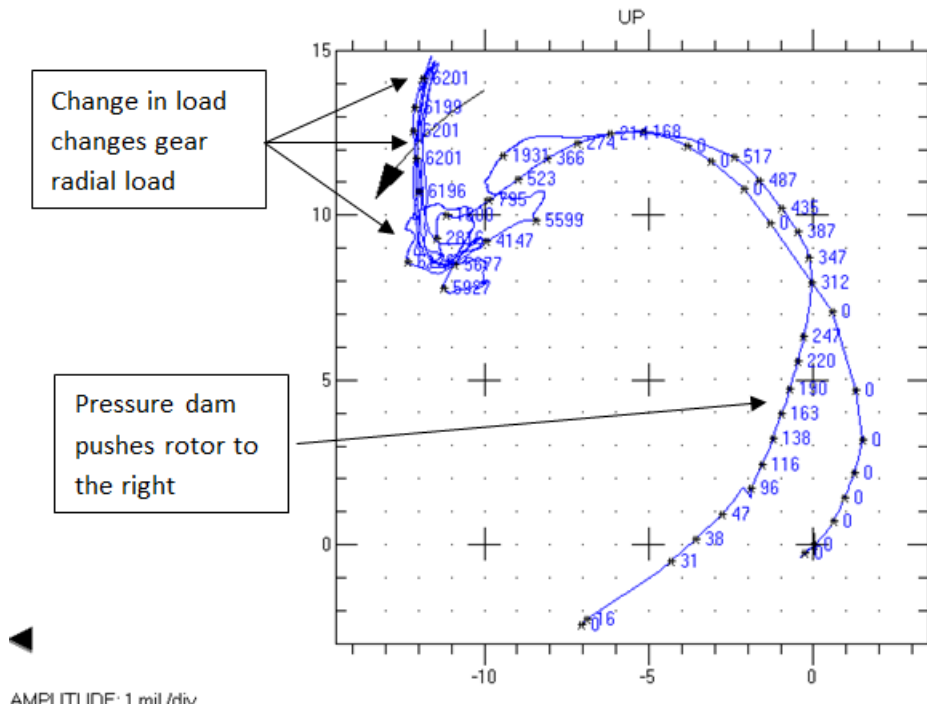
Figure 56. Cascade plot of GTG pinion radial vibration

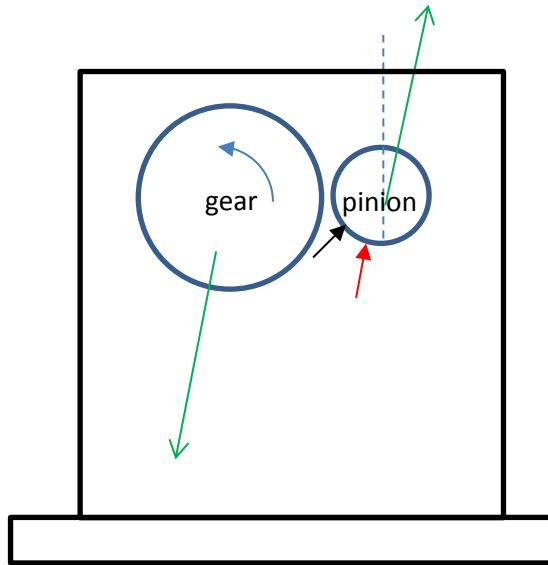*Figure 57. GTG gearbox pinion DE shaft centerline plot*

Figure 58. Generator gearbox showing design gear loads vectors (green), original pressured dam location (black), and modified(red) on pinion
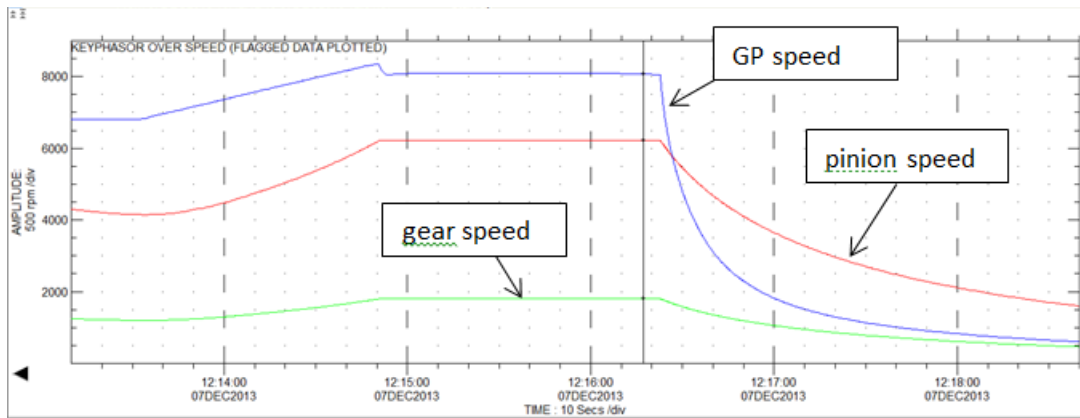

Figure 59. Speed trend during open breaker trip, gas producer(blue), pinion(red), gear(green)
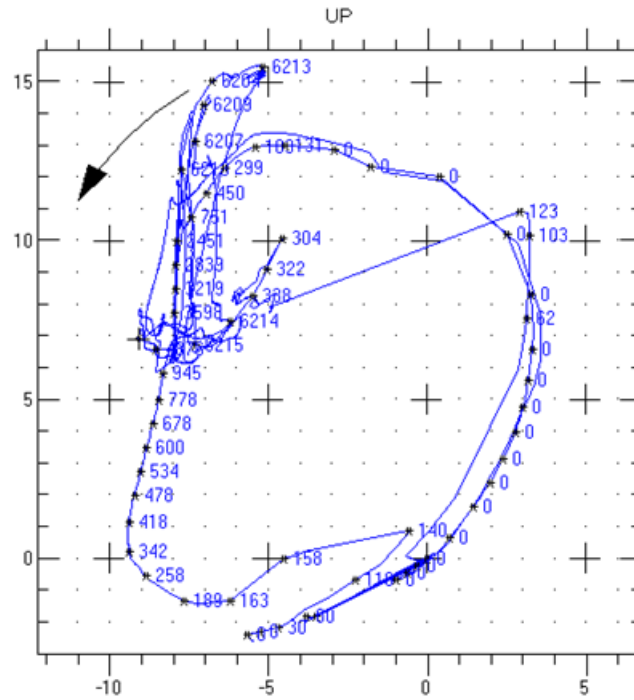
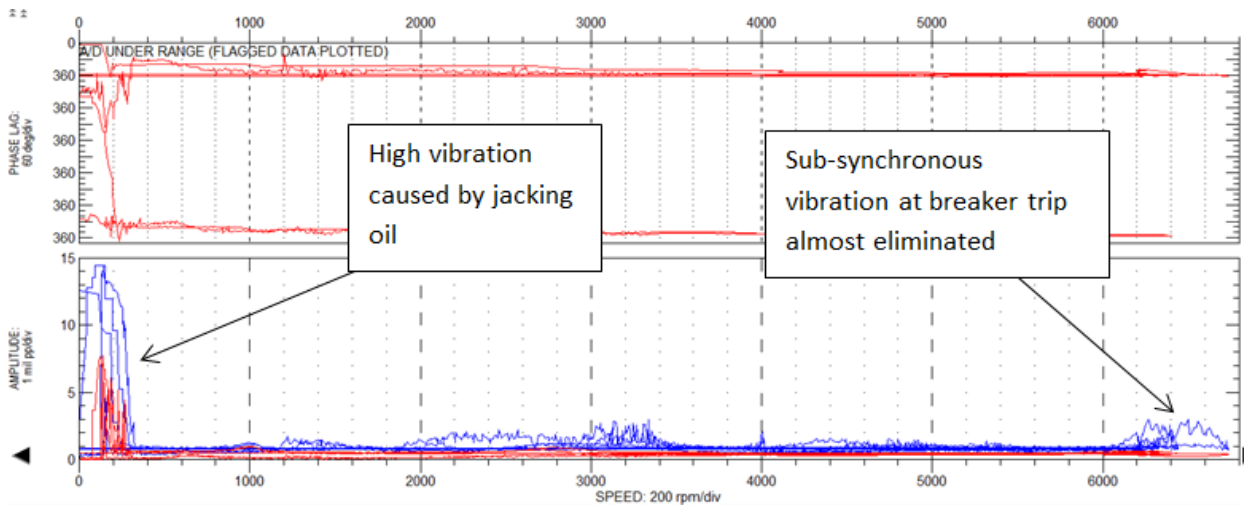*Figure 60. Shaft centerline plot after bearing modification*

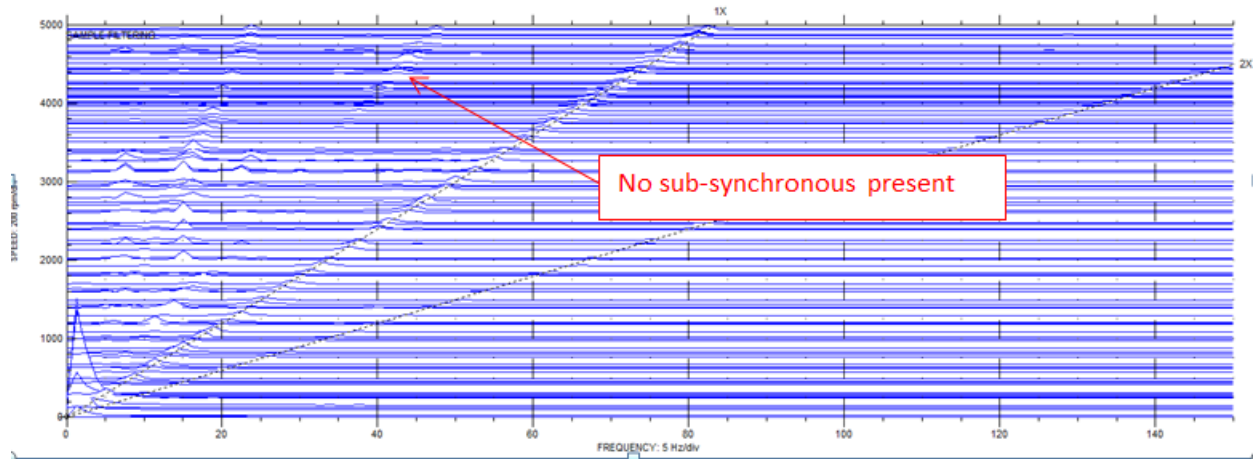*Figure 61. GTG pinon DE radial vibration after bearing modification*

Figure 62. GTG pinion DE cascade plot after bearing modification

SUMMARY

Because of the complexity of modern turbomachinery a higher level of vibration analysis is required. This requires an understanding of the measurement devices, additional plotting options, identification of rotor modes, and basic rotordynamics. The importance of the relative location of the rotor's natural frequencies to the operating speed (i.e. separation margin) was covered and how this may significantly change the produced vibration.

Several examples were provided of the next level of analysis includes identifying natural frequencies or modes of a system to determine if a potential resonance occurs. The complexity of turbomachinery requires this higher level of vibration analysis, which includes understanding the importance of transient data (i.e. start-up/shutdown), the role of rotordynamics, advanced signal processing, and many other concepts. The importance of the measured amplification factor in troubleshooting machinery was covered. Also, "tuning" a rotordynamic model so that it accurately predicts the measured vibration was explained as well.

Bibliography

1. Bently Nevada Training. (1998). *Advanced Machinery Dynamics Course.* Minden, Nevada: Bently Nevada .

2. Childs, D. W. (2013). *Turbomachinery Rotordynamics with Case Studies.* Welborn, Texas: Minter Spring Publishing.

3. Davidson, T. R., Salamone, D. J., & Gunter, E. J. (1992). Rotor Bearing and Shaft Dynamics Redesign of a Double-Overhung Turboexpander for Reliability Improvement. *Proceedings of the Twenty-First Turbomachinery Symposium* (pp. 35-57). College Station, TX: Texas A&M University.

4. Eisenmann, R. C., & Eisenmann, R. C. (1998). *Machinery Malfunction Diagnosis and Correction.* Upper Saddle River, NJ: Prentice-Hall.

5. Jackson, C. (1979). *The Practical Vibration Primer.* Houston: Gulf Publishing Company.

6. Nicholas, J., Edney, S., Matthews, T., & Varela, F. J. (2001). Eliminating a Rub-Induced Start-up Vibration Problem in an Etylene Drive Steam Turbine. *Proceedings of the Fifteenth Turbomachinery Symposium* (pp. 65-79). College Station, TX: Texas A&M University.

7. Nicholas, J., Whalen, J., & Franklin, S. (1986). Improving Critical Speed Calculations using Flexible Bearing Support FRF Compliance Data. *Proceedings of the Thirtieth Turbomachinery Symposium* (pp. 69-78). College Station, TX: Texas A&M University.

8. Vance, J., Zeidan, F., & Murphy, B. (2010). *Machinery Vibration and Rotordynamics.* Hoboken: John Wiley and Sons.

9. Zeidan, F., & Paquette, D. (1994). Application of High Speed and High Performance Fluid Film Bearings in Rotating Machinery. *Proceedings of the Twenty-third Turbomachinery Symposium* (pp. 209-233). College Station, TX: Texas A&M University.